

## Article

# Citrus hystrix Extracts Protect Human Neuronal Cells against High Glucose-Induced Senescence

Nattaporn Pattrachotanant <sup>1,2</sup> and Tewin Tencomnao <sup>1,2,\*</sup>

<sup>1</sup> Department of Clinical Chemistry, Faculty of Allied Health Sciences, Chulalongkorn University, Bangkok 10330, Thailand; nat.ahs11@gmail.com

<sup>2</sup> Age-Related Inflammation and Degeneration Research Unit, Chulalongkorn University, Bangkok 10330, Thailand

\* Correspondence: tewin.t@chula.ac.th; Tel.: +66-2-218-1533

Received: 5 August 2020; Accepted: 23 September 2020; Published: 30 September 2020



**Abstract:** *Citrus hystrix* (CH) is a beneficial plant utilized in traditional folk medicine to relieve various health ailments. The antisenescent mechanisms of CH extracts were investigated using human neuroblastoma cells (SH-SY5Y). Phytochemical contents and antioxidant activities of CH extracts were analyzed using a gas chromatograph–mass spectrometer (GC-MS), 2,2-diphenyl-1-picryl-hydrazyl-hydrate (DPPH) assay and 2,2'-azino-bis (3-ethylbenzthiazoline-6-sulphonic acid) (ABTS) assay. Effects of CH extracts on high glucose-induced cytotoxicity, reactive oxygen species (ROS) generation, cell cycle arrest and cell cycle-associated proteins were assessed using a 3-(4,5-Dimethylthiazol-2-yl)-2,5-diphenyltetrazolium bromide tetrazolium (MTT) assay, non-fluorescent 2', 7'-dichloro-dihydrofluorescein diacetate ( $H_2DCFDA$ ) assay, flow cytometer and Western blot. The extracts protected neuronal senescence by inhibiting ROS generation. CH extracts induced cell cycle progression by releasing senescent cells from the G1 phase arrest. As the Western blot confirmed, the mechanism involved in cell cycle progression was associated with the downregulation of cyclin D1, phospho-cell division cycle 2 (pcdc2) and phospho-Retinoblastoma (pRb) proteins. Furthermore, the Western blot showed that extracts increased Sirtuin 1 (SIRT1) expression by increasing the phosphorylation of Glyceraldehyde 3-phosphate dehydrogenase (GAPDH). Collectively, CH extracts could protect high glucose-induced human neuronal senescence by inducing cell cycle progression and up-regulation of SIRT1, thus leading to the improvement of the neuronal cell functions.

**Keywords:** *Citrus hystrix*; neuronal senescence; high glucose; SIRT1; cyclin D1; pcdc2; pRb; SH-SY5Y

## 1. Introduction

Hyperglycemia is a key characteristic and risk factor that triggers neuronal damage, leads to encephalopathy and causes the development of Diabetes mellitus (DM)-associated neurodegenerative diseases through the induction of neuronal senescence [1–4]. The incidence of most neurodegenerative diseases, such as Alzheimer’s (AD) and Parkinson’s disease (PD), has been shown to increase exponentially with advancing hyperglycemia and neuronal senescence. Hyperglycemia results in damage of brain structure and is closely related with the development of cognitive impairment and dementia, thus increasing amyloid beta accumulation [5]. Hyperglycemia can cause neuroinflammation, oxidative stress and cell cycle arrest. Cell cycle arrest is an important process associated with neuronal senescence. In replicatively senescent cells, the cell cycle is arrested at the G1 and/or G2 phase [6,7]. Cell cycle regulation is very complex and there are many proteins required for cell cycle progression.

Retinoblastoma (Rb) is a tumor suppressor that is a major regulator of the G1/S transition. Rb can be phosphorylated by cyclin/cyclin-dependent kinases (CDKs) and forms a complex transcription

factor E2F to control cell progression through the G1 phase [8]. The ability of phospho-Retinoblastoma (pRb) to control the cell cycle has been attributed to E2F suppression [9].

Moreover, there are many CDKs that control the cell cycle, most prominently among them cdk1 or cell division cycle protein 2 (cdc2). The cdc2 level is high in S and G2 but low in G1. Cdc2 can form a complex with both cyclin A and cyclin B for S phase and G2/M transition control, respectively [10].

Cyclin D1 (G1 cyclin regulatory partner) is an important protein that controls cell cycle progression. Many researches indicated that down-regulation of cyclin D1 causes G1 cell cycle arrest by reducing Rb phosphorylation [11–14].

Sirtuin 1 (SIRT1) is a nicotinamide dinucleotide (NAD<sup>+</sup>)-dependent deacetylases. SIRT1 plays an important role in inhibiting cell senescence and extending the lifespan of organisms [15–17]. Moreover, it is an essential factor in the regulation of many processes in cells such as DNA repair, chromatin structure, metabolism, inflammation and cancer [18].

*Citrus hystrix* (CH), called kaffir lime, is a useful tropical plant native to Southeast Asia. It is a small perennial plant with a hard trunk, smooth bark, smooth trunk and spiny branches. It has green, aromatic and distinctively shaped double leaves. Its fruit is either a single or a bunch. Fresh fruits are rough and green and yellow after ripened. It is commonly used as a very popular ingredient in many dishes. For traditional medicine, whole fruits are used for treating various inflammatory aliments, fever, headache, bad breath, digestion, flu and sore throats [19]. The previous phytochemical report showed that this plant contains various phytoconstituents such as high phenolic, flavonoid, alkaloid, tannins, glycerolglycolipids, tocopherols and furanocoumarins in several parts of CH, such as leaf, peel and juice [20]. These phytochemical compounds exhibited many advantages, such as antioxidant, antibacterial, antifungal, anticholinesterase, anticancer, cardioprotective and antidiabetic activities [21–23].

Phytochemical compounds in CH, including citronellal, citronellol, caryophyllene, nerolidol, phytol, ethyl palmitate, sitosterol and α-terpineol and their beneficial effects have been previously described and prompted this investigation.

Citronellal was effective against several pathogenic bacteria and fungi [24–26]. It had the potential to speed up the healing process of *Candida*-infected wounds in a diabetic mouse model [27] and it could decrease the cholesterol level in rats [28]. Furthermore, it had high antioxidant activities [29].

Citronellol is a natural component of citronella oil. It is widely used as an effective mosquito repellent and is used in perfume and beauty products. Specific pharmacological effects for citronellol include antinociceptive activity and anti-inflammatory effects [30]. It provides neuroprotective activity [31], hypotensive and vasorelaxant effects [32].

Caryophyllene is found in numerous essential oils and has a high potential to treat or prevent hepatic injury and neuroinflammation [33–35].

Nerolidol is found in essential oils of many types of plants and flowers and is known for various medicinal properties, including neuroprotective effects [36], antimicrobial activities [37], anti-biofilm activity [38], anti-fungal activities [39,40].

Phytol is widely used as a food additive and a precursor to phylloquinol (vitamin K), tocopherol (vitamin E) and fatty acid phytyl ester production. In the medicinal field, it exerts an anti-inflammatory effect and redox-protective activity [41].

Ethyl palmitate has anti-inflammatory activities [42].

Sitosterol, a phytosterol (plant sterols), lowers the level of serum low-density lipoprotein cholesterol (LDL-C) and the absorption of intestinal cholesterol [43,44]. It also exerts anti-Alzheimer's activity [45] and antioxidant activity [46,47]. Additionally, it can prevent glutamate and β-amyloid toxicity [48].

α-Terpineol exhibited anti-hypertension, antiproliferation, anti-inflammation, anti-bacteria and antioxidant. Moreover, it could re-establish insulin sensitivity [49–53].

In this study, gallic acid (GA) was used as a positive control. GA has emerged as a strong antioxidant found in fruits and vegetables. GA showed the anti-aging activity on skin [54,55],

anti-senescence accelerated mice [56], anti-dementia [57], anti-diabetes [58,59] and neuroprotective effect [24,60].

The aim of this study was to investigate the mechanism for antisenescent activity of CH extracts on a human neuroblastoma cell line (SH-SY5Y). The advantage may be useful for developing alternative medicines to prevent neuronal senescence.

## 2. Results

### 2.1. Antioxidant Properties and Total Phenolic and Flavonoid Contents

In this study, *Citrus hystrix* peels and leaves were designated as CHP and CHL, respectively. To investigate the free radical scavenging capacities of CHP and CHL, we used a 2,2-diphenyl-1-picryl-hydrazyl-hydrate or DPPH assay, as well as a 2,2'-azino-bis (3-ethylbenzthiazoline-6-sulphonic acid) or ABTS assay. Strong antioxidant activity was found in both CHP and CHL extracts. In CHL extract, we found high phenolic ( $2134.48 \pm 1.06$  mg(GA)/g of dry weigh) and flavonoid ( $2856.15 \pm 1.24$  mg(QE)/g of dry weigh) contents. Table 1 shows free radical scavenging activity data using a DPPH scavenging assay. In Table 2, we show free radical scavenging activity data using an ABTS scavenging assay. Table 3 shows total phenolic and flavonoid content data.

**Table 1.** Free radical scavenging activities of ethanolic extracts of *Citrus hystrix* (CH) using a 2,2-diphenyl-1-picryl-hydrazyl-hydrate (DPPH) scavenging assay.

Sample	% Radical Scavenging Activity (of 1 mg/mL Extract)	mg VCEAC/g Dry Weight Sample
CHP	$14.98 \pm 5.25$	$210.06 \pm 11.95$
CHL	$15.36 \pm 6.79$	$238.89 \pm 12.25$

VCEAC: Vitamin C equivalent antioxidant capacity.

**Table 2.** Free radical scavenging activities of ethanolic extracts of CH using a 2,2'-azino-bis (3-ethylbenzthiazoline-6-sulphonic acid) (ABTS) scavenging assay.

Sample	% Radical Scavenging Activity (of 1 mg/mL extract)	mg VCEAC/g Dry Weight Sample
CHP	$90.38 \pm 0.11$	$3063.67 \pm 3.71$
CHL	$65.18 \pm 0.33$	$2219.99 \pm 11.12$

VCEAC: Vitamin C equivalent antioxidant capacity.

**Table 3.** Total phenolic and flavonoid contents of ethanolic extracts of CH.

Sample	Total Phenolic (mg(GA)/g of Dry Weight)	Total Flavonoid (mg(QE)/g of Dry Weight)
CHP	$1796.55 \pm 1.38$	$1521.54 \pm 3.54$
CHL	$2134.48 \pm 1.06$	$2856.15 \pm 1.24$

GA: Gallic acid; QE: Quercetin.

### 2.2. Phytochemical Constituents of CHP and CHL

The extraction yields of CHP and CHL were 14.17% and 13.04%, respectively. Gas chromatograph-mass spectrometer (GC-MS) analysis showed the presence of different phytochemical compounds in both extracts. All peaks in both CHP and CHL extracts were detected and compared the MS data with databases to identify chromatographic peaks. GC-MS chromatograms of CHP and CHL were shown in Figures 1 and 2. In the percentage of compounds, we identified 18 proposed phytochemical constituents in CHP, which is detailed in Table 4. Moreover, in Table 5, we detail 12 proposed phytochemical constituents in CHL.

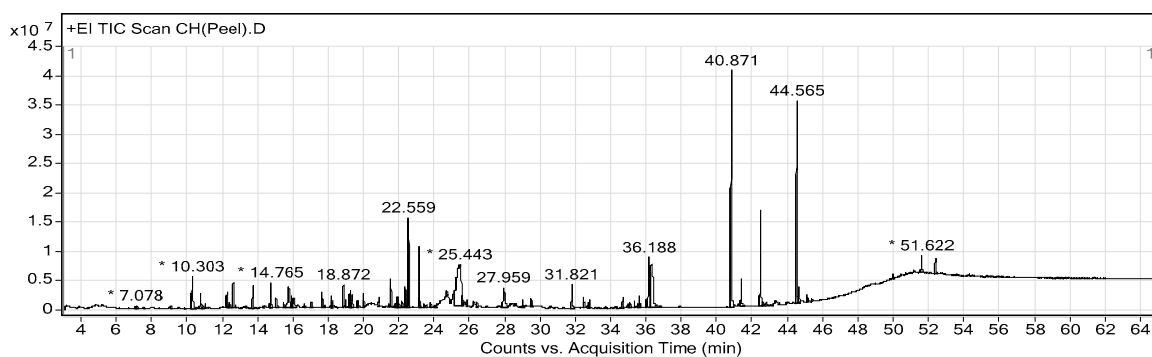


**Figure 1.** Gas chromatograph–mass spectrometer (GC-MS) chromatogram of *Citrus hystrix* peels (CHP). \* Peaks of proposed phytochemical constituents in CHP were suggested by GC-MS.

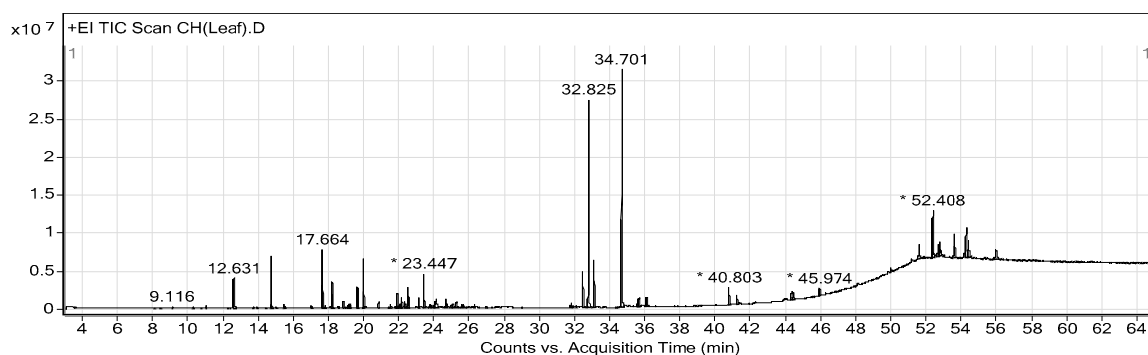


**Figure 2.** GC-MS chromatogram of *Citrus hystrix* leaves (CHL). \* Peaks of proposed phytochemical constituents in CHL were suggested by GC-MS.

**Table 4.** Proposed phytochemical constituents in *Citrus hystrix* peels (CHP) compared with the National Institute of Standards and Technology (NIST) database.

Peak No.	RT	Area (%)	MF	MW	Name of Compound
12	12.635	0.9	C <sub>10</sub> H <sub>18</sub> O	154	Citronellal
15	13.735	0.87	C <sub>10</sub> H <sub>18</sub> O	154	α-Terpineol
18	14.765	1.01	C <sub>10</sub> H <sub>20</sub> O	156	Citronellol
23	16.061	1.08	C <sub>8</sub> H <sub>14</sub> O <sub>3</sub>	158	Methyl 6-oxoheptanoate
30	18.872	0.83	C <sub>15</sub> H <sub>24</sub>	204	α-Copaene
36	20.018	0.58	C <sub>15</sub> H <sub>24</sub>	204	Caryophyllene
40	21.559	1.13	C <sub>15</sub> H <sub>24</sub>	204	β-Cubebene
46	22.558	3.54	C <sub>15</sub> H <sub>24</sub>	204	Cadinene
44	22.2	0.24	C <sub>14</sub> H <sub>22</sub> O	206	Phenol, 2,4-bis(1,1-dimethylethyl)-
61	29.504	0.7	C <sub>9</sub> H <sub>6</sub> O <sub>3</sub>	162	7-Hydroxycoumarin
62	31.821	1.23	C <sub>16</sub> H <sub>32</sub> O <sub>2</sub>	256	n-Hexadecanoic acid
63	32.495	0.39	C <sub>18</sub> H <sub>36</sub> O <sub>2</sub>	284	Hexadecanoic acid, ethyl ester
68	34.698	0.41	C <sub>20</sub> H <sub>40</sub> O	296	Phytol
76	36.32	6.86	C <sub>11</sub> H <sub>6</sub> O <sub>4</sub>	202	7H-Furo(3,2-g)(1)benzopyran-7-one, 9-hydroxy-
77	40.871	14.86	C <sub>16</sub> H <sub>14</sub> O <sub>5</sub>	286	7H-Furo(3,2-g)(1)benzopyran-7-one, 4-(2,3-epoxy-3-methylbutoxy)-, (S)-(—)-
78	41.405	1.37	C <sub>16</sub> H <sub>14</sub> O <sub>5</sub>	286	4-(3-Methyl-2-oxobutoxy)-7H-furo(3,2-g)(1)benzopyran-7-one
82	44.565	12.4	C <sub>16</sub> H <sub>16</sub> O <sub>6</sub>	304	4-(2,3-Dihydroxy-3-methylbutoxy)furo(3,2-g)chromen-7-one
88	52.412	0.81	C <sub>29</sub> H <sub>50</sub> O	414	Sitosterol

RT: retention time; MF: molecular formula; MW: molecular weight.

**Table 5.** Proposed phytochemical constituents in *Citrus hystrix* leaves (CHL) compared with the NIST database.

Peak No.	RT	Area (%)	MF	MW	Name of Compound
9	12.631	2.35	C <sub>10</sub> H <sub>18</sub> O	154	Citronellal
13	14.758	3.53	C <sub>10</sub> H <sub>20</sub> O	156	Citronellol
17	17.664	4.24	C <sub>10</sub> H <sub>20</sub> O <sub>2</sub>	172	Cyclohexanol, 2-(2-hydroxy-2-propyl)-5-methyl-
28	20.014	3.51	C <sub>15</sub> H <sub>24</sub>	204	Caryophyllene
36	22.193	0.78	C <sub>14</sub> H <sub>22</sub> O	206	Phenol, 2,4-bis(1,1-dimethylethyl)-
40	23.447	2.39	C <sub>15</sub> H <sub>26</sub> O	222	1,6,10-Dodecatrien-3-ol, 3,7,11-trimethyl-
55	31.918	0.19	C <sub>20</sub> H <sub>30</sub> O <sub>4</sub>	334	1,2-Benzenedicarboxylic acid, butyl octyl ester
57	32.494	2.52	C <sub>18</sub> H <sub>36</sub> O <sub>2</sub>	284	Hexadecanoic acid, ethyl ester
61	34.701	17.3	C <sub>20</sub> H <sub>40</sub> O	296	Phytol
65	40.803	1.53	C <sub>16</sub> H <sub>14</sub> O <sub>5</sub>	286	7H-Furo(3,2-g)(1)benzopyran-7-one, 4-(2,3-epoxy-3-methylbutoxy)-, (S)-(–)-
68	44.484	0.73	C <sub>16</sub> H <sub>16</sub> O <sub>6</sub>	304	4-(2,3-Dihydroxy-3-methylbutoxy)furo(3,2-g)chromen-7-one
71	52.408	4.91	C <sub>29</sub> H <sub>50</sub> O	414	Sitosterol

RT: retention time; MF: molecular formula; MW: molecular weight.

### 2.3. Neuronal Senescent Model

To create a neuronal senescent model, SH-SY5Y cells were induced into an expression of intracellular reactive oxygen species (ROS) by treating cells with 5.55 (control) to 100 mM glucose. In addition, the effect of glucose on cell viability was detected. We found that glucose could significantly increase the percentage of intracellular ROS in a dose-dependent manner after treatment for 24 h (Figure 3). Moreover, the highest concentration of glucose that had no effect on cell viability was 100 mM (Figure 4). From all results, we used 100 mM glucose to induce neuronal senescence in this model.

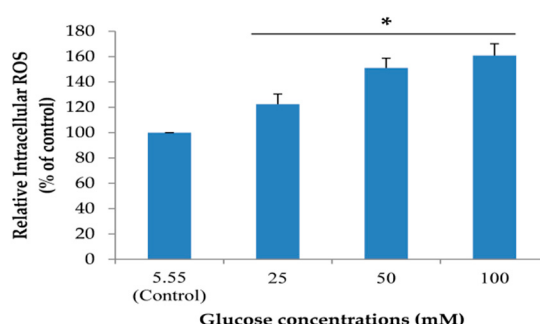


**Figure 3.** The effect of different concentrations of glucose on intracellular reactive oxygen species (ROS). Relative intracellular ROS level was performed using a microplate reader. Data are mean  $\pm$  SD, \*  $p < 0.05$  vs. control.  $p$  values were 0.03, 0.007 and 0.000 for groups treated with glucose concentrations of 25, 50 and 100 mM, respectively.

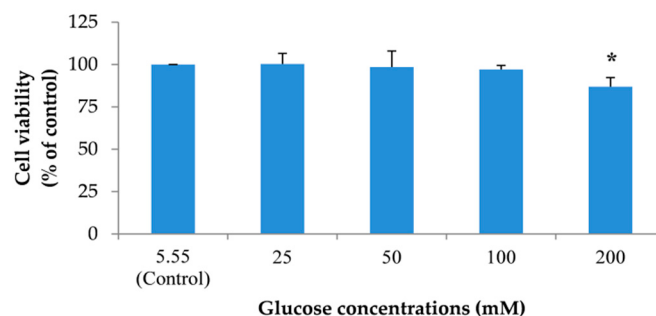


**Figure 4.** The effect of different concentrations of glucose on SH-SY5Y cell viability. Detection of cell viability was performed using 3-(4,5-Dimethylthiazol-2-yl)-2,5-diphenyltetrazolium bromide tetrazolium (MTT) assay. Data are presented as the means  $\pm$  SD, \*  $p < 0.05$  vs. control.  $p$  values of 200 mM glucose-treated group was 0.000.

#### 2.4. Effects of the Extracts on Cell Viability

Using the working concentrations of both extracts, CHP and CHL (0 to 100  $\mu$ g/mL) were prepared. We found that all concentrations of CHL had no effect on cell viability. For the CHP effect, the results showed that CHP at the concentration of 50 and 100  $\mu$ g/mL could significantly decrease cell viability. As seen in Figure 5, the percentage of cell viability treated with CHP for 24 h was  $85.50 \pm 4.56\%$  and  $72.48 \pm 16.12\%$  in 50 and 100  $\mu$ g/mL, respectively.

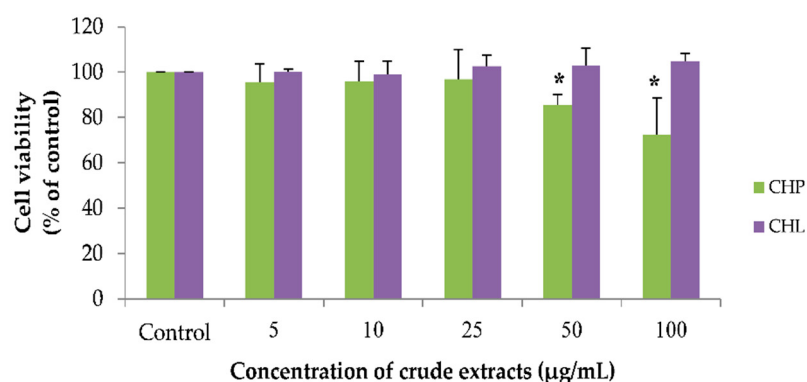


**Figure 5.** The effect of CHP and CHL on cell viability. Detection of cell viability was performed using an MTT assay. Data are presented as the means  $\pm$  SD, \*  $p < 0.05$  vs. control.  $p$  values were 0.018 and 0.030 in groups treated with CHP concentrations of 50 and 100  $\mu$ g/mL, respectively.

#### 2.5. Effects of the Extracts on Intracellular ROS Reduction

To examine the effects of CHP and CHL on high glucose-induced intracellular ROS, this experiment was investigated by treating cells with 100 mM glucose alone or combined with different concentrations of CHP (1, 5 and 10  $\mu$ g/mL) and CHL (1, 5, 10 and 25  $\mu$ g/mL). The dose-response curve of CH extracts was obtained by isovolumetric additions of CHP and CHL solutions of different concentrations so that the DMSO concentration range was from 0.001 to 0.025% ( $v/v$ ). We found that both CHP and CHL at 1  $\mu$ g/mL could significantly reduce the percentage of high glucose-induced intracellular ROS (Figure 6a,b). However, to clarify the effect of DMSO in CH extracts on intracellular ROS accumulation, cells were treated with 0.001 to 0.025% ( $v/v$ ) DMSO alone for 24 h. In the H<sub>2</sub>DCFDA assay, we show that the increasing DMSO alone did not affect ROS generation in SH-SY5Y cells (Figure 6c). This result clarified that both CHP and CHL extracts appeared to be effective reducing the intracellular ROS accumulation at the concentration of 1  $\mu$ g/mL but not at higher concentrations was not caused by DMSO.

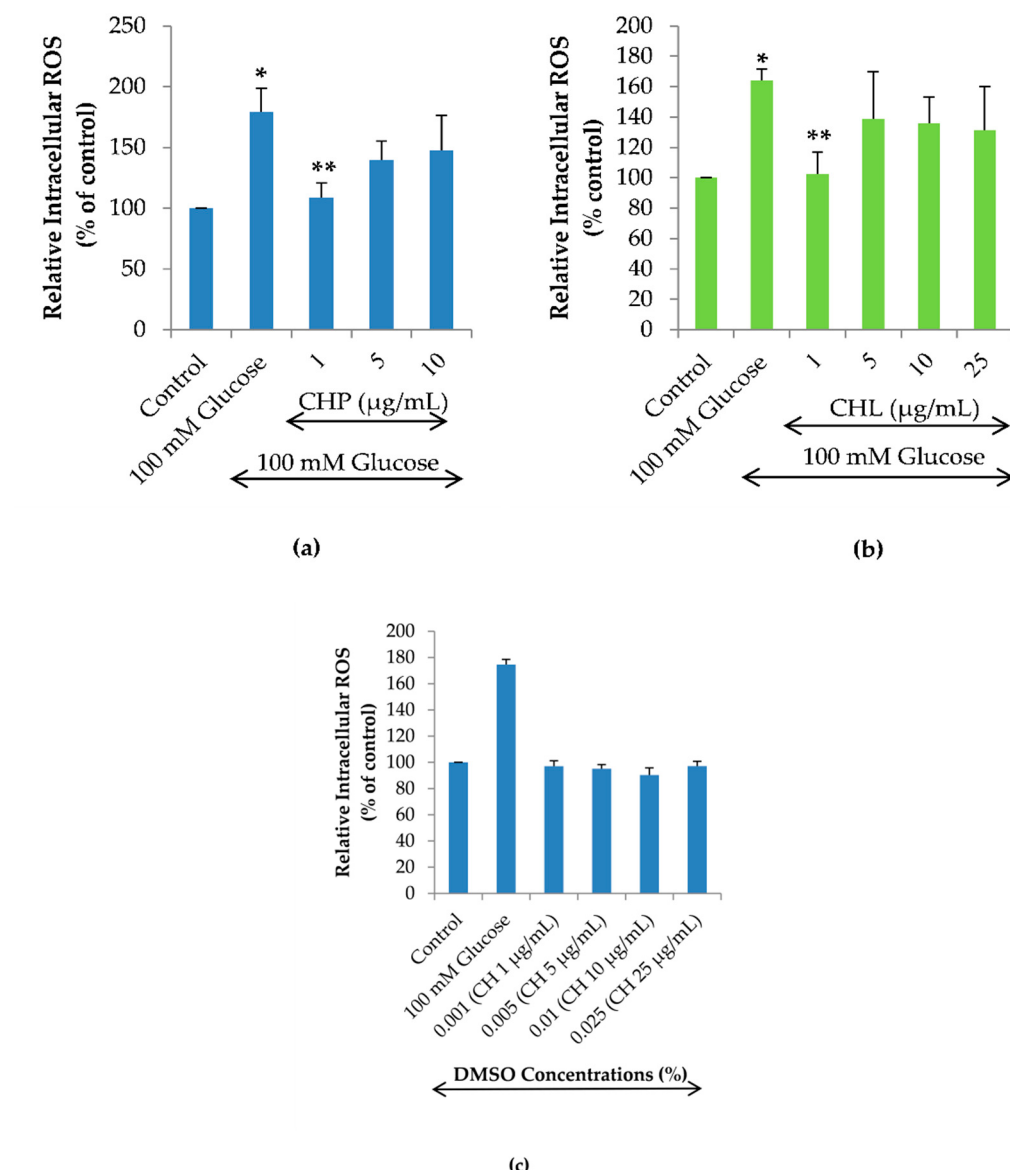
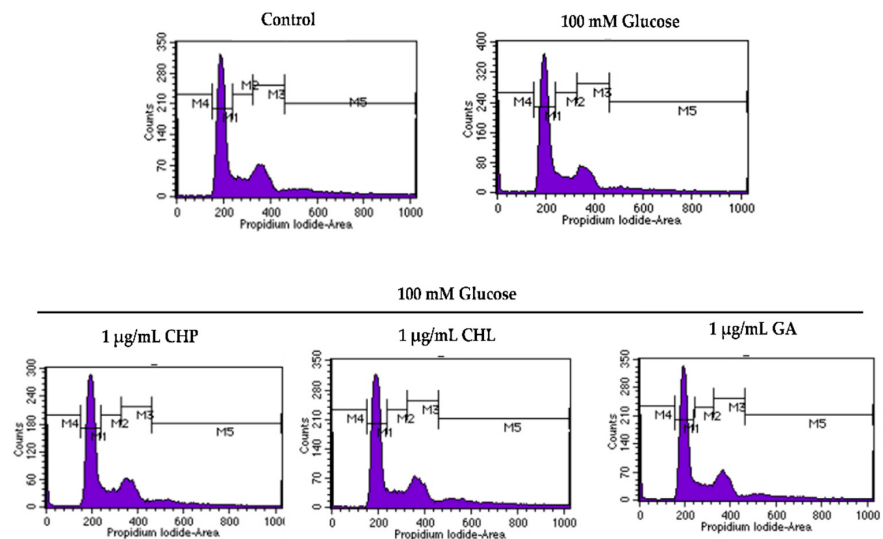


**Figure 6.** Effects of the extracts on high glucose-induced ROS accumulation in SH-SY5Y cells. Relative intracellular ROS level of SH-SY5Y cells treated with 100 mM glucose alone or combined with different concentrations for either CHP (a) or CHL (b) for 24 h. The effect of DMSO on relative intracellular ROS level of SH-SY5Y cells treated with (0.001 to 0.025% (v/v)) DMSO alone (c). Data are presented as the means  $\pm$  SD, \*  $p < 0.05$  vs. control; \*\*  $p < 0.05$  vs. 100 mM glucose alone. For CHP,  $p$  value was 0.002 in both 100 mM glucose and 1  $\mu$ g/mL groups. For CHL,  $p$  value was 0.000 in both 100 mM glucose and 1  $\mu$ g/mL groups.

## 2.6. Effects of the Extracts on Cell Cycle

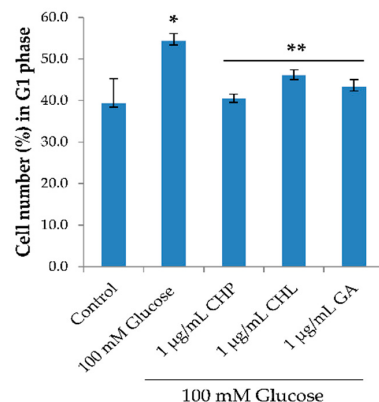
To further understand the ability of both CHP and CHL on neuronal senescence, we determined the activity on cell cycle distribution. Data generated from a flow cytometer demonstrated that the percentage of cells in the G0/G1 phase when treated with 100 mM glucose was significantly higher than in the control group ( $p < 0.05$ ). Moreover, 100 mM glucose arrested cells in the resting phase (G0/G1). The percentage of cells in the G0/G1 phase after treatment combined with 100 mM glucose and 1  $\mu$ M of either extract or gallic acid was significantly decreased when compared with the group treated with glucose ( $p < 0.05$ ) (Figure 7). Gallic acid (GA) was used as a positive control in this study.



(a) Cell cycle histogram.

Cell Population	Control	100 mM Glucose	100 mM Glucose 1 µg/mL CHP	100 mM Glucose 1 µg/mL CHL	100 mM Glucose 1 µg/mL GA
G1	39.36 ± 5.91	54.41 ± 1.69 *	40.55 ± 0.98 **	46.08 ± 1.29 **	43.29 ± 1.78 **
S	11.31 ± 0.9	10.78 ± 1.87	10.34 ± 1.54	11.61 ± 0.33	10.52 ± 1.06
G2/M	31.30 ± 2.53	31.56 ± 1.71	29.27 ± 4.58	29.12 ± 2.04	27.95 ± 0.06

(b) The percentage of cell number



(c) The percentage of cell number

**Figure 7.** The effect of extracts on the cell cycle. Quantitative determination based on propidium iodide (PI) staining was carried out using a flow cytometer. The results showed (a) cell cycle histogram, (b,c) the percentage of cell numbers. Data are presented as the means  $\pm$  SD, \*  $p$  < 0.05 vs. control; \*\*  $p$  < 0.05 vs. 100 mM glucose alone.  $p$  values were 0.001, 0.001, 0.039 and 0.007 for 100 mM glucose, CHP, CHL and GA, respectively.

## 2.7. Effect of the Extracts on Cell Cycle-Associated Protein and SIRT1 Expression

Cell cycle regulation is of critical importance in the senescence process. The cell cycle diagram and the cell numbers carried out in a flow cytometer showed that high glucose may cause cell senescence by interfering cell cycle progression. The extracts could affect high glucose. To confirm this, we investigated the expression of three proteins: cyclin D1 (G1 cyclin regulatory partner),

pRb (G1 checkpoint) and pcdc2 (S and G2 checkpoint) using the Western blot. Figure 8, shows the expression of cyclin D1 and pRb was significantly increased when cells were treated with 100 mM of glucose alone (\*  $p < 0.05$  vs. control). When treated with 1  $\mu$ g/mL of either CHL or GA, both pRb and pcdc2 proteins were significantly decreased and only cyclin D1 expression was reduced in response to treatment with 1  $\mu$ g/mL CHP (\*\*  $p < 0.05$  vs. 100 mM glucose alone).

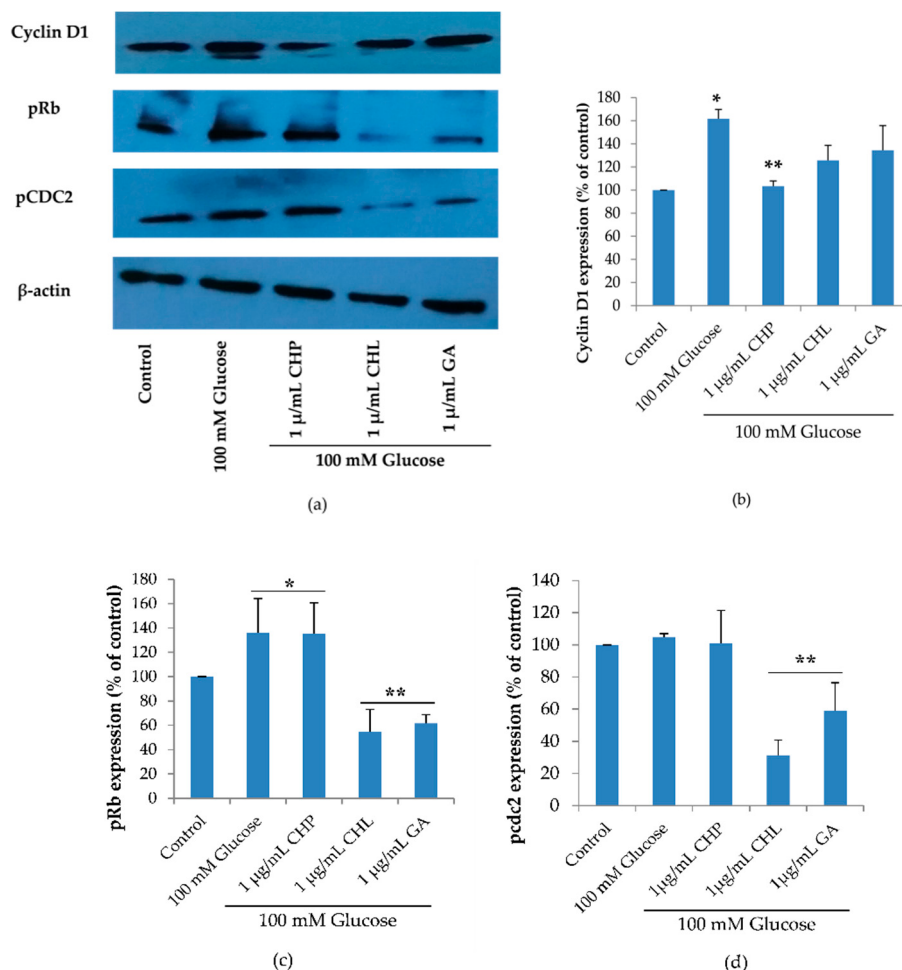


**Figure 8.** Cyclin D1, phospho-Retinoblastoma (pRb) and phospho-cell division cycle 2 (pcdc2) expression, as shown in a representative Western blot (**a**). Normalized values of Cyclin D, pRb and pcdc2 against  $\beta$ -actin ((**b**), (**c**) and (**d**), respectively). The mean  $\pm$  SD values of normalized Cyclin D, pRb and pcdc2 expression were obtained from three independent experiments, \*  $p < 0.05$  vs. control; \*\*  $p < 0.05$  vs. 100 mM glucose alone. For Cyclin D1,  $p$  values were 0.019 and 0.027 for 100mM glucose and CHP, respectively. For pRb,  $p$  values were 0.037, 0.049, 0.001 and 0.002 for 100 mM glucose, CHP, CHL and GA, respectively. For pcdc2,  $p$  values were 0.011 and 0.042 for CHL and GA, respectively.

SIRT1 plays an important role in cell cycle and cell senescence. SIRT1 expression is a response to glucose starvation, as it activates GAPDH phosphorylation. As revealed in Figure 9, SIRT1 and GAPDH expression levels were not significantly different between the control and 100 mM glucose-treated groups. In extract-treated groups, CHP, CHL and GA significantly reduced glucose level in cells. When the glucose level was low, GAPDH was phosphorylated and phospho-GAPDH translocated into a nucleus that up-regulated SIRT1 expression. For these reasons, we found that SIRT1 expression significantly increased and decreased GAPDH expression, which was observed in extract-treated cells (\*\*  $p < 0.05$  vs. 100 mM glucose alone).

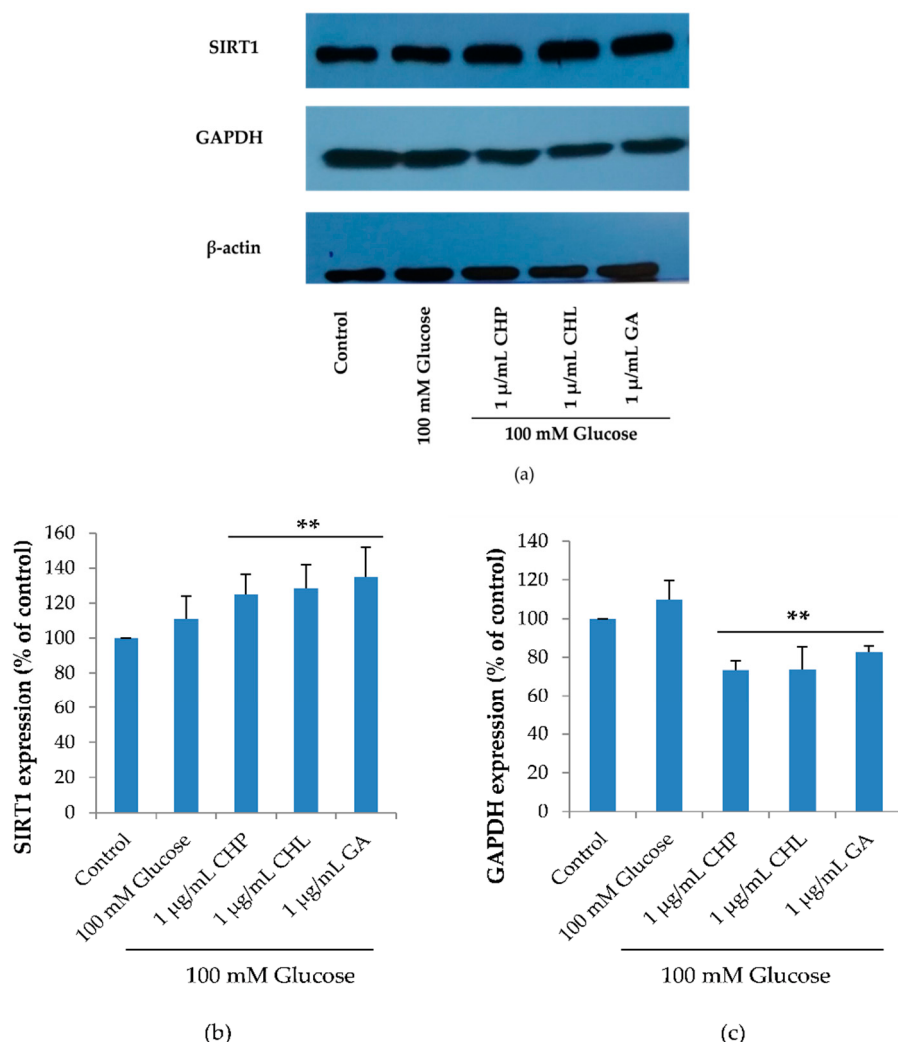


**Figure 9.** Sirtuin 1 (SIRT1) and Glyceraldehyde 3-phosphate dehydrogenase (GAPDH) expression, as shown in a representative Western blot (a). Normalized values of SIRT1 and GAPDH against  $\beta$ -actin ((b) and (c)). The mean  $\pm$  SD values of normalized SIRT1 and GAPDH expression were obtained from three independent experiments, \*  $p < 0.05$  vs. control; \*\*  $p < 0.05$  vs. 100 mM glucose alone. For SIRT1,  $p$  values were 0.005, 0.011 and 0.005 for CHP, CHL and GA, respectively. For GAPDH,  $p$  values were 0.001, 0.001 and 0.008 for CHP, CHL and GA, respectively.

### 3. Discussion

*Citrus hystrix* is a medicinal plant that treats many ailments and it is used in many traditional medicines. Based on DPPH and ABTS assays, high antioxidant properties of its extracts were reported. Furthermore, the phytochemical constituents were analyzed and identified by GC-MS. The spectrum of GC-MS confirmed that CHP and CHL contain a number of various bioactive compounds. The nature and beneficial effects on health of these compounds were discussed in Table 6.

**Table 6.** Compound nature and bioactivity of phytochemical constituents in CHP and CHL.

Name of Compound	Compound Nature	Bioactivity
Citronellal	Monoterpeneoid	Antibacterial and antifungal activities [24,40] Wound healing property on chronic diabetic wounds [27] Relaxing effects [61,62]
Citronellol	Monoterpene alcohol	Anti-inflammatory and analgesic activities [30,63]
Cyclohexanol, 2-(2-hydroxy-2-propyl)-5-methyl-	Monoterpeneoid	Insect repellents [64,65]
Caryophyllene	Monoterpenes	Anti-inflammatory pathologies, atherosclerosis and tumors [35,66,67] Antioxidant activity [68,69] Analgesic activity [70,71]
2,4-bis(1,1-dimethylethyl)Phenol	Phenol	Antioxidant activity [72–74] Anti-inflammatory activity [74,75]
1,6,10-Dodecatrien-3-ol, 3,7,11-trimethyl- or (Nerolidol)	Sesquiterpene alcohol	Antioxidant activity [76–80] Anti-inflammatory and analgesic activities [81,82] Neuroprotective effect [36]
1,2-Benzenedicarboxylic acid, butyloctyl ester	Ester	Antioxidant activity [83]
Hexadecanoic acid, ethyl ester or (Ethyl palmitate)	Palmitic acid ester (Fatty acid ethyl ester)	Antioxidant, hypocholesterolemic, anti-androgenic [84] Anti-inflammatory activities [42]
Phytol	Diterpene alcohol	Antioxidant and neuroprotective effects [41,85]
7H-Furo(3,2-g)(1)benzopyran-7-one, 4-(2,3-epoxy-3-methylbutoxy)-, (S)-(-)- or (Heraclenin)	Furanocoumarin	Anti-inflammatory activity [86]
4-(2,3-Dihydroxy-3-methylbutoxy) furo(3,2-g)chromen-7-one or (Oxypeucedanin hydrate oraviprin)	Furanocoumarin	Antioxidant activity Anticancer activity [87,88]
Sitosterol	Phytosterol	Prevention of the coronary heart disease [43,44] Anti-Alzheimer's activity [45] Antioxidant activity [46,47] Prevention of glutamate and β-amyloid toxicity [48]

Table 6. Cont.

Name of Compound	Compound Nature	Bioactivity
$\alpha$ -Terpineol	Monoterpene alcohol	Antioxidant activity, antiulcer activity Cardiovascular and antihypertensive effects Anticonvulsant and sedative activity Re-establish insulin sensitivity Antibacterial activity Anti-nociceptive activity [49–53]
Methyl 6-oxoheptanoate	Methyl ester	Anticancer activity [89]
$\alpha$ -Copaene	Sesquiterpene	Antioxidant and anticancer activities [90,91]
Cadinene	Sesquiterpene	Antioxidant activity [92]
7-Hydroxycoumarin or Umbelliferon	Coumarin	Antihyperlipidemic and antidiabetic effects [93,94] Anti-inflammatory and antioxidant activities [95,96] Neuroprotective effect [97–99]
n-Hexadecanoic acid	Palmitic acid	Anti-inflammatory and antioxidant activities [84,100]
7H-Furo(3,2-g)(1)benzopyran-7-one, 9-hydroxy- or (Xanthotoxol)	Furanocoumarin	Antioxidant activity and neuroprotective effect [101,102]
4-(3-Methyl-2-oxobutoxy)-7H-furo(3,2-g)(1)benzopyran-7-one or (Isooxypeucedanin)	Furanocoumarin	Antidiabetic effects [103]

Hyperglycemia is a major cause of diabetes-associated neuronal diseases through cellular senescence. Cellular senescence is the process of an irreversible cell cycle arrest through many mechanisms, that is, inflammation cytokine, oxidative stress and cell cycle checkpoint [104–106]. Further, it causes many age-related chronic diseases such as atherosclerosis, Alzheimer’s disease and cancer [107–111]. The antidiabetic and antioxidant activity of CH and its phytochemical constituents was described earlier in human adipocytes, cataract in streptozotocin-induced diabetic rats [112] and hepatoprotective effect in paracetamol-induced injury in rats [23]. However, the exact pathway of protective effect of CH on high glucose-induced neuronal senescence was not explored.

Interestingly, CHP and CHL extracts appeared to effectively reduce the intracellular ROS accumulation at the concentration of 1  $\mu$ g/mL but not at higher concentrations. Notably, it is interesting that CHP and CHL may also possess a pro-oxidant activity when administered at high doses. It is worth noting that contributing factors such as dosage, phytochemical profile and oxidation-reduction potential (ORP) may relate to the balance between the beneficial and deleterious activities [113]. The detail of ORP is described herein biochemical perspective.

Given the effectiveness of both CHP and CHL to decrease ROS induced by high glucose, we hypothesized that both extracts may provide neuronal cell protection against cell cycle arrest induced by high glucose. To test our hypothesis, we first analyzed cell cycle via a flow cytometer.

For flow cytometry results (Figure 7a,b), the percentage of cells at the G1 phase in the 100 mM glucose-treated group significantly increased compared with the control group. In addition, both CHP and CHL extracts significantly decreased the percentage of the cell number in the G1 phase.

To further confirm the effect of CHP and CHL on cell cycle, the expression of cell cycle checkpoint proteins (pRb and cdc2), cyclin D1 and SIRT1 was detected by the Western blot.

Checkpoint processes control the cell cycle to avoid the accumulation of genetic damage. It does so by monitoring DNA integrity and cell growth during G1/S and G2/M transitions. These processes are common to all eukaryotic cells [114]. As Figure 10 shows, in the early and middle points of the G1 phase, Rb binds to E2F causing cells to arrest. However, in late stage of the G1 phase, Rb is phosphorylated by CDKs to increase gene transcription and permit cells to enter the S phase. Cyclin/cdc2 complexes control the cell cycle. Cdc2 is high in the S and G2 phases. In the S phase, G2/M transition control binds to cyclin A and cyclin B, respectively. Cyclin/cdc2 complexes are inactive due to Wee1/Myt1 phosphorylation.

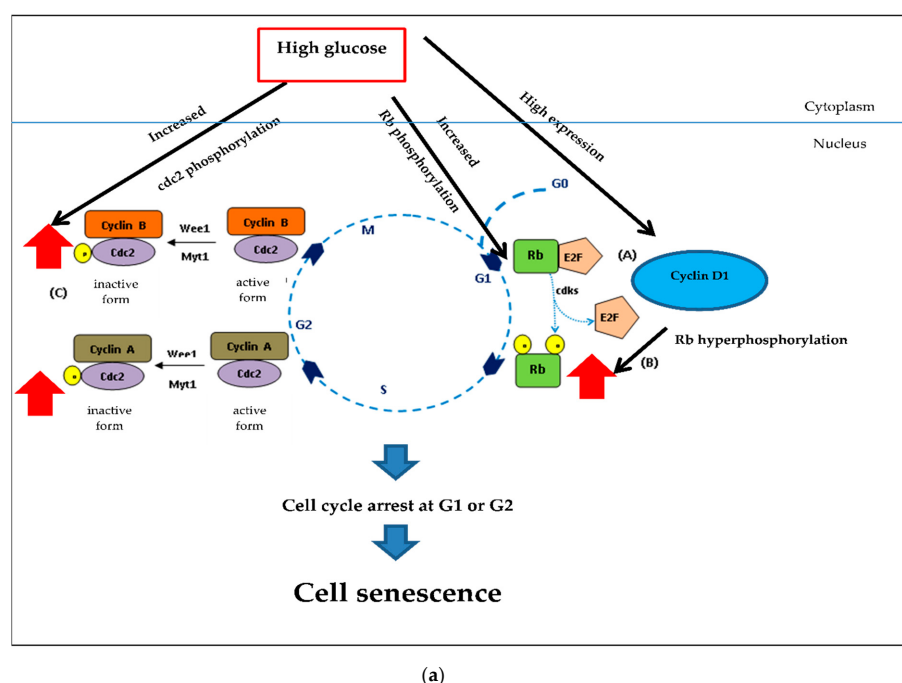
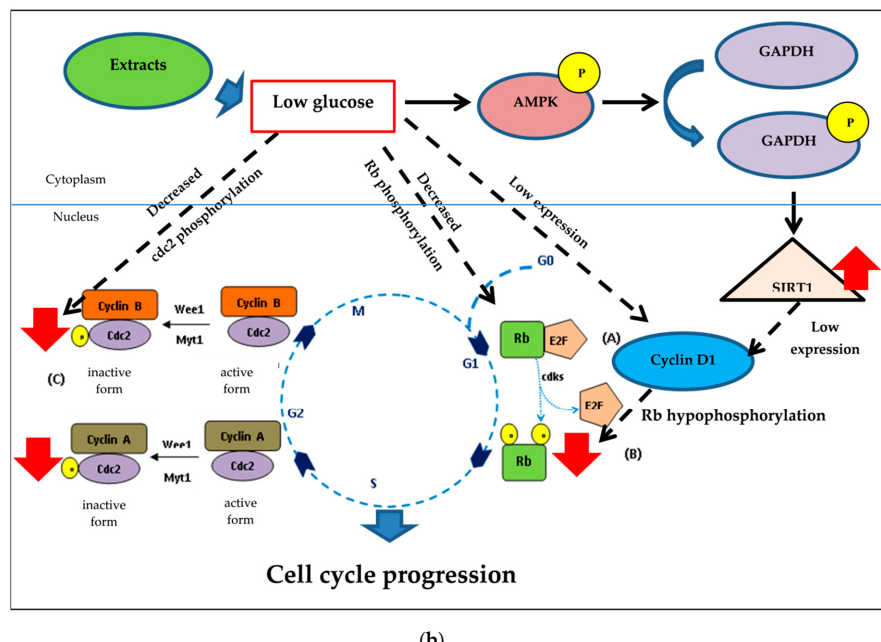


Figure 10. Cont.



**Figure 10.** Underlying mechanisms of CHP and CHL exerts and their anti-senescence activity in SH-SY5Y cells. (a) In hyperglycemia, hyperphosphorylation of Rb induced by high glucose and cyclin D1 caused cell cycle arrest at G1. Hyperphosphorylated Rb failed to assemble with E2F. Furthermore, pcdc2 was an inactive form that caused cell cycle arrest. (b) Both extracts could reduce high glucose level. Low cellular glucose significantly increased GAPDH phosphorylation via AMP-activated protein kinase (AMPK), triggering SIRT1 activation. This mechanism induced the cell cycle progression by decreasing Rb and cdc2 phosphorylation. High expression of proteins ( $\uparrow$ ); Low expression of proteins ( $\downarrow$ ); Hyperphosphorylation of proteins ( $\rightarrow$ ); Hypophosphorylation of proteins ( $\leftarrow$ ).

The Western blot results demonstrated that high glucose significantly increased cyclin D1, pRb and pcdc2. Increased cyclin D1 could induce phosphorylation of Rb (Figure 10a). Although the pRb/E2F complex permits cell progression in the G1 and S phase, in hyperglycemia, hyperphosphorylation of Rb-induced high glucose and cyclin D1 caused cell cycle arrest at G1. Many studies have indicated that hyperphosphorylated Rb failed to assemble E2F [115–117]. Furthermore, we found pcdc2 to be an inactive form that caused cell cycle arrest.

Although both CHP and CHL were similarly effective in reducing ROS accumulation, they exerted neuronal cell protection against cell cycle arrest induced by high glucose through different signaling pathways. We observed that CHP significantly decreased only cyclin D1 expression in extract-treated groups, while CHL significantly decreased both pRb and pcdc2 expression. However, taken together, our results showed that both CHP and CHL could provide neuronal cell protection against cell cycle arrest induced by high glucose.

Noticeably, the difference of the effect on cell-cycle associated protein expression between CHP-treated and CHL-treated groups might be due to the compositional differences of the two extracts, as shown by the GC-MS analysis. GC-MS analysis (Tables 4 and 6) revealed that phytochemical constituents of isooxypeucedanin,  $\alpha$ -terpineol and umbelliferone were only found in CHP and exerted antidiabetic effect by normalizing blood glucose level and re-establishing insulin sensitivity [57,58,66]. The previous studies showed the effect of certain antidiabetic drugs on the cell-cycle through the decrease of cyclin D1 expression [118]. Cyclin D1 is an essential link between cell-cycle and energy control metabolism [119]; this may explain why CHP was only effective in reducing cyclin D1 protein expression but not pRb and pcdc2 expression.

SIRT1 is an important protein that plays a role in cell senescence. We hypothesized that both CHP and CHL could protect cell senescence by up-regulating SIRT1 expression. The Western blot results confirmed our hypothesis. When cells were treated with either CHP or CHL, SIRT1 expression was significantly up-regulated.

Furthermore, we hypothesized that SIRT1 would up-regulate through the phosphorylation of GAPDH. GAPDH and SIRT1 expression, when treated with either CHP or CHL, confirmed that both extracts could reduce the glucose level in cells. Figure 10b showed the underlying mechanisms of both extracts. Low cellular glucose significantly increased the phosphorylation of GAPDH and SIRT1 expression. When cellular glucose decreased, GAPDH became a critical enzyme and was phosphorylated by AMP-activated protein kinase (AMPK), thus triggering SIRT1 activation. This process was necessary to protect cells from glucose starvation, such as autophagy and gluconeogenesis [120]. Results from the Western blot showed the association of SIRT1 and cyclin. These results are consistent previous studies, that is, down-regulated SIRT1 was arrested in the G1 phase via cyclin D1 signaling [121,122].

Thus, all results showed that both CHP and CHL could attenuate high glucose-induced cellular senescence in human neuronal SH-SY5Y cells by inducing the cell cycle progression and up-regulation of SIRT1.

In this study, we found CH extracts with high ROS-scavenging properties and they were able to protect high glucose-induced human neuronal senescence. The antioxidant and anti-senescence properties of CH extracts are also extensively discussed in further characterization from two perspectives.

### 3.1. A Biochemical Perspective

Notably, in this study, radical scavenging activity assays of CHP and CHL extracts dissolved in DMSO were performed with DPPH and ABTS in ethanol. However, it still needs to be established whether CHP and CHL extracts' radical scavenging activities could persist in living tissues' aqueous environment under physiological conditions. CH extracts should be administered to animals treated with high glucose to induce senescence. Followed by CH's biochemical evaluation on oxidative stress in blood and tissue samples should be investigated to clarify whether CHP and CHL have scavenging activities under physiological conditions. For example, using samples derived from blood or tissues, antioxidant biomarkers (such as Glutathione (GSH)) could be analyzed. The GSH content indicates the cell's defense against ROS causing cellular injury [123,124] and reflecting the ability of a tissue to scavenge excess superoxide anions leading to oxidative stress [125], Malondialdehyde (MDA)-a direct indicator of cell membrane damage occurring in the tissue [126,127], Catalase (CAT)-an indicator of CH toleration by that particular tissue [128], Superoxide dismutase (SOD)-an indicator of the active enzyme involvement in neutralizing the effect of free radicals [129] and Level of protein content-an indicator of cell capacity of mitigating the effect of free radical and peroxide processes resulting in modulating the cellular antioxidant status [130]. Furthermore, other aspects, as below, are also concerned as described below [131,132].

- Therapeutic agents with high lipid solubility can penetrate cells more rapidly than therapeutic agents with water solubility. So, lipid or water solubility should be assessed.
- Most of the therapeutic agents are available as weak acids or weak bases. Thus the pH of therapeutic agents should be addressed appropriately.
- Oxidation-reduction potential (ORP) [133], also known as redox, should be determined because it reflects a molecule's ability to oxidize or reduce another molecule. Reducers have negative ORP and oxidizers have positive ORP. Typically, all organs in our body have negative ORP (-10 to -250 mV of ORP). Oxidizers can oxidize another molecule, which causes it to lose electrons. Oxidizers become free radicals after accepting radicals and cause many diseases. On the other hand, free radicals can be neutralized with reducers and antioxidants, causing body improvement and rejuvenation. For medicinal benefits, CH or their major active constituents should have

negative ORP and play a role as a reducer or antioxidant. Therefore, the proposed application of redox reactions is useful for CH determination in pharmaceuticals (Figure 11).

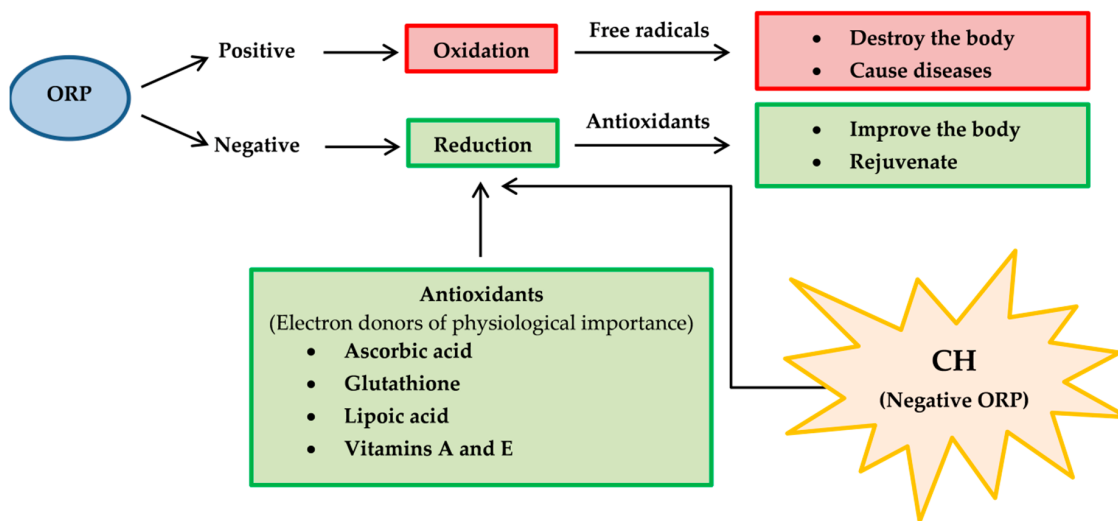


**Figure 11.** The potential applications of oxidation-reduction potential (ORP) or redox reaction for CH determination in pharmaceuticals.

- Oxygen partial pressure ( $\text{PO}_2$ ) [134]:  $\text{PO}_2$  is the force exerted by oxygen. In the human body (highly aerobic organism), oxygen plays a role in energy production. Therefore, oxygen supply at the tissue must match metabolic demand.  $\text{PO}_2$  is useful to maintain homeostasis (the balance between oxygen delivery and its consumption) within organ and tissue. Each organ and tissue has its  $\text{PO}_2$  requirements in order to function correctly.  $\text{PO}_2$  is useful in predicting oxygen and oxygen movement will move from a higher  $\text{PO}_2$  area to a lower  $\text{PO}_2$  area. Typically,  $\text{PO}_2$  in tissue is low because oxygen is used in cellular respiration. When  $\text{PO}_2$  in tissue increased by several factors such as stress, anesthesia, tumor and diabetes, oxygen availability is low or hypoxia. In consideration of CH's pharmacology, the importance of hypoxia as below is concerned [135].
  1. Hypoxia may alter the therapeutic effectiveness and metabolism of CH.
  2. Hypoxia may alter cellular function.
  3. Hypoxia may potentiate or mitigate CH-induced toxicity.
  4. CH may potentiate or protect against hypoxia-induced pathology.
  5. CH may alter the relative coupling of blood flow and energy metabolism in an organ.

### 3.2. A Pharmacokinetic Perspective

It is universally agreed before any novel bioactive compound considered a lead for developing an active principle of any preventive or therapeutic usefulness, it is essential to conduct exhaustive animal and pre-clinical studies. Therefore, pharmacokinetic evaluations of CH extracts' active phytochemicals should be studied in animal models including, blood samples for absorption studies, tissues such as intestine, liver, lungs, kidney and heart distribution studies and urine and excreta collection for excretion studies. After sample preparation, extraction of bioactive markers and assessment of pharmacokinetic parameters as listed below should be carried out [136]. The proposed pharmacokinetic diagram after administering the active phytochemical of CH extracts in an animal model is shown in Figure 12.

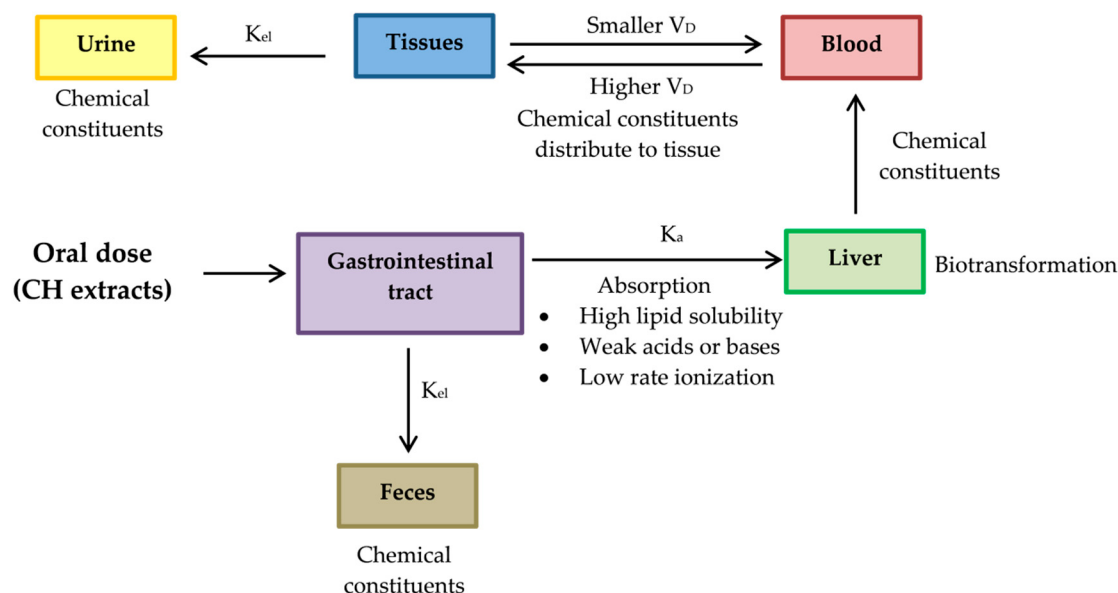


**Figure 12.** The proposed diagram of pharmacokinetics for evaluating of active phytochemicals of CH extracts. After chemical constituents are absorbed by gastrointestinal tract, they are delivered to liver, where they are biotransformed and delivered into blood. Chemical constituents are biodistributed to other peripheral organs by blood stream. Absorbed chemical constituents are excreted through the urine but certain chemical constituents that are not absorbed through the gastrointestinal tract will be eliminated through feces. Absorption rate constant ( $K_a$ ); Constant elimination ( $K_{el}$ ); Volume of distribution ( $V_D$ ).

- Absorption rate constant ( $K_a$ ) should be determined for a chemical compound of CH. The compound investigated should have high  $K_a$ , so its characteristics should be high lipid solubility, weak acids or weak bases and low rate ionization.
- Constant elimination ( $K_{el}$ ) is a value that describes the rate at which an active compound of CH is removed from the human system. Its value is affected by all processes such as distribution, biotransformation and excretion.
- Volume of distribution ( $V_D$ ) represents the distribution of a compound of CH in body tissues rather than the plasma. If  $V_D$  is higher than the total body water, it indicates a greater amount of tissue distribution. A smaller  $V_D$  means a compound remains in the plasma than CH distribution in tissues [137]. A compound studied for medicinal benefits should have higher  $V_D$ , so it should be characterized by high lipid solubility, low rates of ionization and low plasma protein binding capabilities.
- Biotransformation represents the chemical alteration process of therapeutic agents in the body.

As far as pharmacokinetics is concerned, individual chemical constituents found in CH were previously studied, such as sitosterol [138] and caryophyllene [139].

#### 4. Materials and Methods

##### 4.1. Chemicals and Reagents

Dimethyl sulfoxide (DMSO) and ethanol were purchased from Merck (Darmstadt, Germany). Phenylmethyl sulphonyl fluoride (PMSF) was purchased from United States Biological (Cleveland, OH, USA). Kodak processing chemicals were used for autoradiography films. The Amersham ECL select Western blotting detection reagent was purchased from GE Healthcare (Piscataway, NJ, USA). Dulbecco's modified Eagle medium (DMEM)/low glucose, fetal bovine serum (FBS) and penicillin-streptomycin solution (10,000 units/mL of penicillin and 10,000 µg/mL of streptomycin) were

purchased from HyClone (Logan, UT, USA). A solution of 30% acrylamide/bis-acrylamide (37.5:1) was purchased from Biorad (Hercules, CA, USA). Ammonium persulfate (APS) was purchased from EMD Millipore (Billerica, MA, USA). The monoclonal rabbit SIRT1 (D1D7, cat#9475), GAPDH (14C10, cat#2118), Cyclin D1 (92G2, cat#2978), Phospho-Rb (Ser807/811, cat#9308), Phospho-cdc2 (Tyr15, cat#9111) and  $\beta$  actin (13E5, cat#4970) were purchased from Cell Signaling Technology (Beverly, MA, USA). Propidium iodide (PI) was purchased from Biolegend (San Diego, CA, USA).

#### 4.2. Plant Extraction

*Citrus hystrix* (or kaffir lime) peels and leaves were designated as CHP and CHL, respectively and were cultivated in the Bang Ramat District, Taling Chan County and Bangkok, Thailand (Latitude, Longitude: 13.777883, 100.416748). They were harvested in October and November 2019. They were extracted by maceration method using 70% ethanol (ratio 1:5 w/v) at room temperature (RT) in the dark for 48 h and filtered. The residue was extracted twice. The two filtrates were combined and concentrated by evaporation at 45 °C. The crude extracts were dissolved in DMSO or kept at –80 °C until further investigation.

#### 4.3. Gas Chromatograph–Mass Spectrometer (GC-MS) Analysis

The extracts were submitted to the Scientific and Technological Research Equipment Center (STREC) (Chulalongkorn University, Thailand). The GC-MS Triple Quad system was an Agilent 7890 series GC system coupled with an Agilent 7000C MS and a capillary column (HP-5MS 5% Phenyl Methyl Siloxane, length 30 m, i.d. 0.25 mm, phase thickness 0.25  $\mu$ m). The GC was operated with helium as the carrier gas (1 mL/min). The inlet had a temperature of 250 °C, pressure set to 8.2317 psi and 1.5  $\mu$ L injection. The GC oven was kept at 60 °C for 3 min before rising to 325 °C (with linear gradient of 5 °C/min) and kept at 325 °C for 3 min. The total run time was 14 min. The extracts (~10 mg) were dissolved in 1 mL of absolute ethanol and their obtained spectra were compared with NIST Mass Spectrometry Data Center to identify phytochemical constituents.

#### 4.4. Antioxidant Determination

##### 4.4.1. Folin–Ciocalteu Phenol Assay (FCP)

The extracts (50  $\mu$ L) and 10% Folin–Ciocalteu Phenol reagent (50  $\mu$ L) were mixed and incubated in the dark at room temperature (RT) for 30 min. A sodium carbonate ( $\text{Na}_2\text{CO}_3$ ) solution (35  $\mu$ L) was added, mixed and incubated in the dark at RT for 20 min. Reaction absorbance was measured using the Enspire® Multimode Plate Reader (Perkin-Elmer) at 750 nm. Gallic acid was used as the standard. The amount of phenolic compound was in a Gallic acid equivalent (GE) mg/g of dry weight.

##### 4.4.2. Total Flavonoid of Determination

The extracts (50  $\mu$ L) were mixed with the solution (150  $\mu$ L of ethanol, 10  $\mu$ L of 1M Sodium acetate ( $\text{NaOAc}$ ) and 10  $\mu$ L of Aluminum Chloride ( $\text{AlCl}_3$ )). The mixture was incubated in the dark at RT for 40 min and measured at 415 nm. Quercetin was used as the standard. The content of flavonoid was in Quercetin equivalent (QE) mg/g of dry weight.

##### 4.4.3. Radical Scavenging Activity Assays

Next, 0.2 mg/mL of 2,2-diphenyl-1-picryl-hydrazyl-hydrate (DPPH $^\bullet$ ) and freshly prepared 2,2'-azino-bis (3-ethylbenzthiazoline-6-sulphonic acid) (ABTS $^{\bullet+}$ ) ( $\text{OD}_{734} = 0.7\text{--}0.8$ ) were diluted in ethanol. The extract (1 mg/mL) was reacted with DPPH $^\bullet$  or ABTS $^{\bullet+}$  and incubated at RT for 15 and 30 min, respectively. Absorbance was measured at 517 nm and 734 nm, respectively. Ascorbic acid (Vitamin C) was used as the standard for both assays. The antioxidant capacity had Vitamin C equivalent antioxidant capacity (VCEAC) in mg/g of dry weight.

#### 4.5. Cell Line

SH-SY5Y cells—a human neuroblastoma cell line—were purchased from a cell line service (Heidelberg, Germany; Catalogue number 300154). They were cultured in DMEM/low glucose (HyClone, USA) containing 10% FBS and antibiotics (100 U/mL penicillin and 100 µg/mL streptomycin) at 37 °C in a humidified atmosphere at 5% CO<sub>2</sub>.

#### 4.6. 3-(4,5-Dimethylthiazol-2-yl)-2,5-diphenyltetrazolium bromide tetrazolium (MTT) Assay

We determined the nontoxic concentration of CHP and CHL extracts with SH-SY5Y. Cells were seeded at 20,000 cells/well plates and incubated at 37 °C for 24 h. Cells were treated with various concentrations of extracts for 24 h. MTT (5 mg/mL) was added to each well (20 µL/well) and incubated for 4 h. Media was removed carefully. In this step, a formazan product was formed and dissolved with 150 µL of 100% DMSO. A supernatant was collected and transferred to a new 96-well plate. Moreover, it measured the absorbance with a spectrometer at 550 nm. The nontoxic concentration of the extracts was shown as the percentage of cell viability calculated by the following formula.

$$\% \text{ cell viability} = \frac{(\text{Abs}_{\text{treated cells}} - \text{Abs}_{\text{blank}}) \times 100}{\text{Abs}_{\text{untreated cells}} - \text{Abs}_{\text{blank}}}$$

#### 4.7. Reactive Oxygen Species (ROS) Assay

The appropriate concentration of extracts was tested. Cells were seeded at 20,000 cells/well in 96-well plates and incubated at 37 °C for 24 h. Cells were treated or co-treated with 100 mM glucose or extracts for 24 h. Next, 5 µM of non-fluorescent 2',7'-dichloro-dihydrofluorescein diacetate (H<sub>2</sub>DCFDA) was loaded, incubated at 37 °C for 45 min and then washed 3 times with PBS. The level of intracellular ROS was measured based on the ability of ROS to oxidize non-fluorescent H<sub>2</sub>DCFDA into a highly fluorescent 2',7'-dichlorofluorescein (DCF). The fluorescence was measured with an excitation wavelength of 485 nm and an emission wavelength of 535 nm.

#### 4.8. Cell Cycle Assay by Flow Cytometer

Cells were seeded at 500,000 cells/well in 6-well plates and incubated at 37 °C for 24 h. Having been incubated, cells were co-treated with 100 mM glucose and 1 µg/mL of CHP, CHL or gallic acid for 24 h. After treatment, cells were harvested, washed in cold PBS and re-centrifuged at 400 g for 5 min. Cells were re-suspended in absolute ethanol at –20 °C for at least 2 h. Cells were washed and re-suspended in 1% (v/v) Triton X-100 PBS and treated with RNase. Next, 500 µL of PI/Triton X-100 staining solution was added and incubated at 37 °C for 15 min. The cell cycle was analyzed via flow cytometry (FACSCalibur (BD Biosciences, San Jose, CA, USA)).

#### 4.9. Protein Expression by Western Blotting

Cells were seeded at 500,000 cells/well in 6-well plates and incubated at 37 °C for 24 h. Cells were co-treated for 24 h. The next day, protein extraction was carried out using 1 mM of PMSF in a NP-40 lysis buffer. Total protein (40 µg) was mixed with a 2× Laemmli buffer (ratio 1:1) and heated at 95 °C for 10 min. Protein was separated with 10% sodium dodecyl sulfate-polyacrylamide gel electrophoresis (SDS-PAGE) and transferred onto polyvinylidene difluoride (PVDF) membranes. Membranes were blocked with 5% nonfat milk for 1 h at room temperature. Membranes were incubated with primary antibodies (cyclin D1 (1:2000), pRb (1:2000), pc当地2 (1:2000), SIRT 1 (1:2000), GAPDH (1:10,000) and β actin (1:2000)) overnight at 4 °C. After incubation, membranes were washed 3 times with 1× TBS-Tween 20 (TBST) for 15 min, incubated with secondary antibodies (anti-rabbit IgG, HRP-linked antibody) for 45 min at RT and washed 3 times with TBST for 15 min. Protein bands were visualized by adding an enhanced chemiluminescence detection reagent using autoradiography films and Kodak processing chemicals. Each band was normalized against β actin as an internal control.

#### 4.10. Statistical Analysis

Data were presented as the mean  $\pm$  standard deviation (SD). Means were from at least three independent experiments. Data were analyzed via a one-way analysis of variance (ANOVA) followed by a post hoc Tukey test ( $p$  value  $< 0.05$ ) using low glucose-treated cells as the control group.

### 5. Conclusions

In summary, our results demonstrate that CH is an interesting plant with rich antioxidant properties and bioactive compounds. Both CHP and CHL can protect human neuronal cells from glucose-induced neuronal senescence. The neuroprotective effect of CHP and CHL is mediated through cell cycle progression in cell cycle checkpoint proteins and SIRT1 up-regulation after SIRT1/GAPDH pathway activation. CH extracts could be developed as agents for the protection of high glucose-induced neuronal senescence.

However, the bioactivities of this extract needs to be further explored in other living organisms. Hopefully, neuronal senescence-associated diseases will be clarified in further investigations.

**Author Contributions:** N.P. designed and performed the experiments, analyzed and discussed the data and wrote the paper; T.T. conducted the critical revision and consulted the data. All authors have read and agreed to the published version of the manuscript.

**Funding:** This research was funded by the grant from Age-Related Inflammation and Degeneration Research Unit. This research project is supported by the Second Century Fund (C2F), Chulalongkorn University.

**Acknowledgments:** The authors would like to acknowledge the staff of Division of Allergy and Clinical Immunology, Faculty of Medicine, Chulalongkorn University for allowing the authors to access the flow cytometry facility and the staff of Scientific and Technological Research Equipment Centre (STREC), Chulalongkorn University to analyze phytochemical constituents by Gas Chromatograph-Mass Spectrometer. We would like to express our gratitude to James M. Brimson (Department of Clinical Chemistry, Faculty of Allied Health Sciences, Chulalongkorn University) for his help in English editing and proofreading.

**Conflicts of Interest:** The authors declare no conflict of interest.

### References

- Wu, L.; Chen, Y.; Wang, C.Y.; Tang, Y.Y.; Huang, H.L.; Kang, X.; Li, X.; Xie, Y.R.; Tang, X.Q. Hydrogen sulfide inhibits high glucose-induced neuronal senescence by improving autophagic flux via up-regulation of SIRT1. *Front. Mol. Neurosci.* **2019**, *12*, 1–13. [[CrossRef](#)]
- Fan, F.; Liu, T.; Wang, X.; Ren, D.; Liu, H.; Zhang, P.; Wang, Z.; Liu, N.; Li, Q.; Tu, Y.; et al. CLC-3 expression and its association with hyperglycemia induced HT22 hippocampal neuronal cell apoptosis. *J. Diabetes Res.* **2016**, *2016*, 1–12. [[CrossRef](#)]
- Sima, A.A.; Kamiya, H.; Li, Z.G. Insulin, C-peptide, hyperglycemia, and central nervous system complications in diabetes. *Eur. J. Pharmacol.* **2004**, *490*, 187–197. [[CrossRef](#)]
- Reno, C.M.; Tanoli, T.; Bree, A.; Daphna-Iken, R.; Cui, C.; Maloney, S.E.; Wozniak, D.F.; Fisher, S.J. Antecedent glycemic control reduces severe hypoglycemia-induced neuronal damage in diabetic rats. *Am. J. Physiol. Metab.* **2013**, *304*, 1331–1337. [[CrossRef](#)] [[PubMed](#)]
- Lee, H.J.; Seo, H.I.; Cha, H.Y.; Yang, Y.J.; Kwon, S.H.; Yang, S.J. Diabetes and Alzheimer’s Disease: Mechanisms and Nutritional Aspects. *Clin. Nutr. Res.* **2018**, *7*, 229–240. [[CrossRef](#)] [[PubMed](#)]
- Mao, Z.; Ke, Z.; Gorbunova, V.; Seluanov, A. Replicatively senescent cells are arrested in G1 and G2 phases. *Aging* **2012**, *4*, 431–435. [[CrossRef](#)]
- Stein, G.H.; Dulic, V. Origins of G1 arrest in senescent human fibroblasts. *BioEssays* **1995**, *17*, 537–543. [[CrossRef](#)] [[PubMed](#)]
- Giacinti, C.; Giordano, A. RB and cell cycle progress. *Oncogene* **2006**, *25*, 5220–5227. [[CrossRef](#)] [[PubMed](#)]
- Brown, V.D.; Phillips, R.A.; Gallie, B.L. Cumulative Effect of Phosphorylation of pRB on Regulation of E2F Activity. *Mol. Cell. Biol.* **1999**, *19*, 3246–3256. [[CrossRef](#)]
- Draetta, G.; Luca, F.; Westendorf, J.; Brizuela, L.; Ruderman, J.; Beach, D. Cdc2 protein kinases complexed with both cyclin A and B: Evidence for proteolytic inactivation of MPF. *Cell* **1989**, *56*, 829–838. [[CrossRef](#)]

11. Yang, K.; Hitomi, M.; Stacey, D.W. Variations in cyclin D1 levels through the cell cycle determine the proliferative fate of cell. *Cell Div.* **2006**, *1*, 32. [[CrossRef](#)] [[PubMed](#)]
12. Rezaei, P.F.; Fouladdel, S.; Ghaffari, S.M.; Amin, G.; Azizi, E. Induction of G1 cell cycle arrest and cyclin D1 down-regulation in response to pericarp extract of *Baneh* in human breast cancer T47D cells. *DARU J. Pharm. Sci.* **2012**, *20*, 101. [[CrossRef](#)] [[PubMed](#)]
13. Masamha, C.P.; Benbrook, D.M. Cyclin D1 degradation is sufficient to induce G1 cell cycle arrest despite constitutive expression of cyclin E2 in ovarian cancer cells. *Cancer Res.* **2009**, *69*, 6565–6572. [[CrossRef](#)] [[PubMed](#)]
14. Baldin, V.; Lukas, J.; Marcote, M.J.; Pagano, M.; Draetta, G. Cyclin D1 is a nuclear protein required for cell cycle progression in G1. *Genes Dev.* **1993**, *7*, 812–821. [[CrossRef](#)] [[PubMed](#)]
15. Lee, S.H.; Lee, J.H.; Lee, H.Y.; Min, K.J. Sirtuin signaling in cellular senescence and aging. *BMB Rep.* **2019**, *52*, 24–34. [[CrossRef](#)] [[PubMed](#)]
16. Lamichane, S.; Baek, S.H.; Kim, Y.J.; Park, J.H.; Lamichane, B.D.; Jang, W.B.; Ji, S.T.; Lee, N.K.; Dehua, L.; Kim, D.Y.; et al. MHY2233 attenuates replicative cellular senescence in human endothelial progenitor cells via SIRT1 signaling. *Oxidative Med. Cell. Longev.* **2019**. [[CrossRef](#)]
17. Wang, Y.; Liang, Y.; Vanhoutte, P.M. SIRT1 and AMPK in regulating mammalian senescence: A critical review and a working model. *FEBS Lett.* **2010**, *585*, 986–994. [[CrossRef](#)]
18. Liu, T.F.; McCall, C.E. Deacetylation by SIRT1 reprograms inflammation and cancer. *Genes Cancer* **2013**, *4*, 135–147. [[CrossRef](#)]
19. Hutadilok-Towatana, N.; Chaiyamutti, P.; Panthong, K.; Mahabusarakam, W.; Rukachaisirikul, V. Antioxidative and Free Radical Scavenging Activities of Some Plants Used in Thai Folk Medicine. *Pharm. Biol.* **2006**, *44*, 221–228. [[CrossRef](#)]
20. Abirami, A.; Nagarami, G.; Siddhuraju, P. The medicinal and nutritional role of underutilized citrus fruit *Citrus hystrix* (Kaffir lime): A review. *Drug Invent. Today* **2014**, *6*, 1–5.
21. Irawaty, W.; Ayucitra, A. Assessment on antioxidant and in vitro antidiabetes activities of different fractions of *Citrus hystrix* peel. *Int. Food Res. J.* **2018**, *6*, 2467–2477.
22. Abirami, A.; Nagarami, G.; Siddhuraju, P. In vitro antioxidant, anti-diabetic, cholinesterase and tyrosinase inhibitory potential of fresh juice from *Citrus hystrix* and *C. maxima* fruits. *Food Sci. Hum. Wellness* **2014**, *3*, 16–25. [[CrossRef](#)]
23. Abirami, A.; Nagarami, G.; Siddhuraju, P. Hepatoprotective of leaf extracts from *Citrus hystrix* and *C. maxima* against paracetamol induced liver injury in rat. *Food Sci. Hum. Wellness* **2015**, *4*, 35–41. [[CrossRef](#)]
24. Taweechaisupapong, S.; Aromdee, C.; Khunkitti, W. Antibacterial activity of citronella oil solid lipid particles in oleogel against Propionibacterium acnes and itschemical stability. *Int. J. Essent. Oil Ther.* **2008**, *2*, 167–171.
25. Pattnaik, S.; Vemulpad, S.; Kole, C. Antibacterial and Antifungal activity of ten essential oils in vitro. *Microbios* **1996**, *86*, 237–246. [[PubMed](#)]
26. Jantamas, S.; Matan, N.; Aewsiri, T. Improvement of antifungal activity of Citronella oil against *Aspergillus flavus* on rubberwood (*Hevea Brasiliensis*) using heat curing. *J. Trop. For. Sci.* **2016**, *28*, 39–47.
27. Kandimalla, R.; Kalita, S.; Choudhury, B.; Dash, S.; Kalita, K.; Kotoky, J. Chemical Composition and Anti-Candidiasis Mediated Wound Healing Property of *Cymbopogon nardus* Essential Oil on Chronic Diabetic Wounds. *Front. Pharmacol.* **2016**, *7*, 1–8.
28. Batubara, I.; Suparto, I.H.; Sa'diah, S.; Matsuoka, R.; Mitsunaga, T. Effects of Inhaled Citronella oil and Related Compounds on Rat Body Weight and Brown Adipose Tissue Sympathetic Nerve. *Nutrients* **2015**, *7*, 1859–1870. [[CrossRef](#)]
29. Wasito, W.; Noorhamdani, N.; Sukardi, S.; Suratmo, S. Assessment of antioxidant activity of citronellal extract and fractions of essential oils of *Citrus hystrix* DC. *Trop. J. Pharm. Res.* **2018**, *17*, 1119–1125. [[CrossRef](#)]
30. Santos, P.L.; Matos, J.P.S.C.F.; Picot, L.; Almeida, J.R.G.S.; Quintans, J.S.S.; Quintans-Junior, L.J. Citronellol, a monoterpene alcohol with promising pharmacological activities—A systematic review. *Food Chem. Toxicol.* **2018**, *123*, 459–469. [[CrossRef](#)]
31. De Sousa, D.P.; Goncalves, J.C.R.; Quintans-Junior, L.; Cruz, J.S.; Araujo, D.A.M.; de Almeida, R.N. Study of anticonvulsant effect of citronellol, a monoterpene alcohol, in rodents. *Neurosci. Lett.* **2006**, *401*, 231–235. [[CrossRef](#)] [[PubMed](#)]

32. Bastos, J.F.; Moreira, I.J.; Ribeiro, T.P.; Medeiros, I.A.; Antoniolli, A.R.; de Sousa, D.P.; Santos, M.R. Hypotensive and vasorelaxant effects of citronellol, a monoterpenic alcohol, in rats. *Basic Clin. Pharmacol. Toxicol.* **2009**, *106*, 331–337. [CrossRef] [PubMed]
33. Varga, Z.V.; Matyas, C.; Erdelyi, K.; Cinar, R.; Nieri, D.; Chicca, A.; Nemeth, B.T.; Paloczi, J.; Lajtos, T.; Corey, L.; et al.  $\beta$ -Caryophyllene protects against alcoholic steatohepatitis by attenuating inflammation and metabolic dysregulation in mice. *Br. J. Pharmacol.* **2018**, *175*, 320–334. [CrossRef] [PubMed]
34. Medeiros, R.; Passos, G.F.; Vitor, C.E.; Koepf, J.; Mazzuco, T.L.; Pianowski, L.F.; Campos, M.M.; Calixto, J.B. Effect of two active compounds obtained from the essential oil of *Cordia verbenacea* on the acute inflammatory responses elicited by LPS in the rat paw. *Br. J. Pharmacol.* **2007**, *151*, 618–627. [CrossRef]
35. Ojha, S.; Javed, H.; Azimullah, S.; Haque, M.E. Beta-Caryophyllene, a phytocannabinoid attenuates oxidative stress, neuroinflammation, glial activation, and salvages dopaminergic neurons in a rat model of Parkinson disease. *Mol. Cell. Biochem.* **2016**, *418*, 59–70. [CrossRef] [PubMed]
36. Neto, J.N.; de Almeida, A.; da Silva Oliveira, J.; dos Santos, P.; de Sousa, D.; de Freitas, R. Antioxidant effects of nerolidol in mice hippocampus after open field test. *Neurochem. Res.* **2013**, *38*, 1861–1870. [CrossRef]
37. Hada, T.; Shiraishi, A.; Furuse, S.; Inoue, Y.; Hamashima, H.; Matsumoto, Y.; Masuda, K.; Shiojima, K.; Shimada, J. Inhibitory effects of terpenes on the growth of *Staphylococcus aureus*. *Nat. Med.* **2003**, *57*, 64–67.
38. Lee, K.; Lee, J.H.; Kim, S.I.; Cho, M.; Lee, J. Anti-biofilm, anti-hemolysis, and anti-virulence activities of black pepper, cananga, myrrh oils, and nerolidol against *Staphylococcus aureus*. *Appl. Microbiol. Biotechnol.* **2014**, *98*, 9447–9457. [CrossRef]
39. Curvelo, J.A.R.; Marques, A.M.; Barreto, A.L.S.; Romanos, M.T.V.; Portela, M.B.; Kaplan, M.A.C.; Soares, R.M.A. A novel nerolidol-rich essential oil from *Piper clausenianum* modulates *Candida albicans* biofilm. *J. Med. Microbiol.* **2014**, *63*, 697–702. [CrossRef]
40. Park, M.J.; Gwak, K.S.; Yang, I.; Kim, K.W.; Jeung, E.B.; Chang, J.W.; Choi, I.G. Effect of citral, eugenol, nerolidol and  $\alpha$ -terpineol on the ultrastructural changes of *Trichophyton mentagrophytes*. *Fitoterapia* **2009**, *80*, 290–296. [CrossRef]
41. Renan, O.S.; Sousa, F.B.M.; Damasceno, S.R.B.; Carvalho, N.S.; Silva, V.G.; Oliviera, F.R.; Sousa, D.P.; Aragao, K.S.; Barbosa, A.L.R.; Freitas, R.M.; et al. Phytol, a diterpene alcohol, inhibits the inflammatory response by reducing cytokine production and oxidative stress. *Fundam. Clin. Pharmacol.* **2014**, *4*, 455–464.
42. Saeed, N.M.; El-Demerdash, E.; Abdel-Rahman, H.M.; Algandaby, M.M. Anti-inflammatory activity of methyl palmitate and ethyl palmitate in different experimental rat models. *Toxicol. Appl. Pharmacol.* **2012**, *264*, 84–93. [CrossRef]
43. Plat, J.; Mensink, R.P. Effects of plant sterols and stanols on lipid metabolism and cardiovascular risk. *Nutr. Metab. Cardiovasc. Dis.* **2001**, *11*, 31–40.
44. Gylling, H.; Plat, J.; Turley, S.; Ginsberg, H.N.; Ellegrård, L.; Jessup, W.; Jones, P.J.; Lütjohann, D.; Maerz, W.; Masana, L.; et al. Plant sterols and plant stanols in the management of dyslipidaemia and prevention of cardiovascular disease. *Atherosclerosis* **2014**, *232*, 346–360. [CrossRef] [PubMed]
45. Ayaz, M.; Junaid, M.; Ullah, F.; Subhan, F.; Sadiq, A.; Ali, G.; Ovais, M.; Shahid, M.; Ahmad, A.; Wadood, A.; et al. Anti-Alzheimer's Studies on  $\beta$ -Sitosterol Isolated from *Polygonum hydropiper* L. *Front. Pharmacol.* **2017**, *8*. [CrossRef] [PubMed]
46. He, C.; Li, W.; Zhang, J.J.; Qu, S.S.; Wang, L.Y. Determination of  $\beta$ -Sitosterol and Total Sterols Content and Antioxidant Activity of Oil in Acai (*Euterpe Oleracea*). *China J. Chin. Mater. Med.* **2014**, *39*, 4620–4624.
47. Yoshida, Y.; Niki, E. Antioxidant effects of phytosterol and its components. *J. Nutr. Sci. Vitaminol.* **2003**, *49*, 277–280. [CrossRef]
48. Brimson, J.M.; Brimson, S.J.; Brimson, C.A.; Rakshitawathana, V.; Tencomnao, T. *Rhinacanthus nasutus* extracts prevent glutamate and amyloid- $\beta$  neurotoxicity in HT-22 mouse hippocampal cells: Possible active compounds include lupeol, stigmasterol and  $\beta$ -sitosterol. *Int. J. Mol. Sci.* **2012**, *13*, 5074–5097. [CrossRef]
49. Sabino, C.K.; Ferreria-Filho, E.S.; Mendes, M.B.; Da SilvaFilho, J.C. Cardiovascular effects induced by  $\alpha$ -terpineol in hypertensive rats. *Flavour Frag. J.* **2013**, *28*, 333–339. [CrossRef]
50. Adorjan, B.; Buchbauer, G. Biological properties of essential oils: An update review. *Flavour Frag. J.* **2010**, *25*, 407–426. [CrossRef]
51. Khaleel, C.; Tabanca, N.; Buchbauer, G.  $\alpha$ -Terpineol, a natural monoterpenic alcohol: A review of its biological properties. *Open Chem.* **2018**, *16*, 349–361.

52. De Sousa, G.M.; Cazarin, C.B.B.; Junior, M.R.M.; Lamas, C.A.; Quitete, V.H.A.C.; Pastore, G.M.; Bicas, J.L. The effect of  $\alpha$ -terpineol enantiomers on biomarkers of rats fed a high-fat diet. *Heliyon* **2020**, *6*, e03752. [[CrossRef](#)]
53. Srisukh, V.; Tribuddharat, C.; Nukoolkarn, V.; Bunyapraphatsara, N.; Chokephaibulkit, K.; Phoomniyom, S.; Chaunphung, S.; Srifuengfung, S. Antibacterial activity of essential oils from *Citrus hystrix* (makrut lime) against respiratory tract pathogens. *Science* **2012**, *38*, 212–217.
54. Chaikul, P.; Khat-Udomkiri, N.; Iangthanarat, K.; Manosroi, J.; Manosroi, A. Characteristics and in vitro anti-skin aging activity of gallic acid loaded in cationic CTAB noisome. *Eur. J. Pharm. Sci.* **2019**, *131*, 39–49. [[CrossRef](#)] [[PubMed](#)]
55. Hwang, E.; Park, S.Y.; Lee, H.J.; Lee, T.Y.; Sun, Z.W.; Yi, T.H. Gallic acid regulates skin photoaging in UVB-exposed fibroblasts and hairless mice. *Phytother. Res.* **2014**, *28*, 1778–1788. [[PubMed](#)]
56. Li, L.; Ng, T.B.; Gao, W.; Li, W.; Fu, M.; Niu, S.M.; Zhao, L.; Chen, R.R.; Liu, F. Antioxidant activity of gallic acid from rose flowers in senescence accelerated mice. *Life Sci.* **2005**, *77*, 230–240.
57. Hajipour, S.; Sarkaki, A.; Farbood, Y.; Eidi, A.; Mortazavi, P.; Valizadeh, Z. Effect of gallic acid on dementia type of Alzheimer disease in rats: Electrophysiological and Histological studies. *Basic Clin. Neurosci.* **2015**, *7*, 97–106.
58. Patel, S.S.; Goyal, R.K. Cardioprotective effects of gallic acid in diabetes-induced myocardial dysfunction in rats. *Pharmacogn. Res.* **2011**, *3*, 239–245.
59. Elahi, E.; Ashfaq, A.; Mustafa, S. Impact of gallic acid on oxidative stress in diabetes. *PJMHS* **2018**, *12*, 80–82.
60. Shabani, S.; Rabiee, Z.; Amini-Khoei, H. Exploring the multifaceted neuroprotective actions of gallic acid: A review. *Int. J. Food Prop.* **2020**, *23*, 736–752.
61. Saeki, Y.; Shiohara, M. Physiological effects of inhaling fragrances. *Int. J. Aromather.* **2001**, *11*, 118–125. [[CrossRef](#)]
62. Sayowan, W.; Siripornpanich, V.; Piriyapunyaporn, T.; Hongratanaworakit, T.; Kotchabhakdi, N.; Ruangrungsi, N. The Harmonizing Effects of Citronella Oil on Mood States and Brain Activities. *J. Health Res.* **2012**, *26*, 69–75.
63. Brito, R.G.; Guimaraes, A.G.; Quintans, J.S.; Santos, M.R.V.; De Sousa, D.P.; Badaue-Passos, D., Jr.; de Lucca, W., Jr.; Brito, F.A.; Barreto, E.O.; Oliviera, A.P.; et al. Citronellol, a monoterpenic alcohol, reduces nociceptive and inflammatory activities in rodents. *J. Nat. Med.* **2012**, *66*, 637–644. [[CrossRef](#)] [[PubMed](#)]
64. Drapeau, J.; Rossano, M.; Touraud, D.; Obermayr, U.; Geier, M.; Rose, A.; Kunz, W. Green synthesis of para-Menthane-3,8-diol from *Eucalyptus citriodora*: Application for repellent products. *C. R. Chim.* **2011**, *14*, 629–635. [[CrossRef](#)]
65. Carroll, S.P.; Loyer, J. PMD, a Registered Botanical Mosquito Repellent with Deet-Like Efficacy. *J. Am. Mosq. Control Assoc.* **2006**, *22*, 507–514. [[CrossRef](#)]
66. Chang, H.J.; Kim, J.M.; Lee, J.C.; Kim, W.K.; Chun, H.S. Protective effect of beta-caryophyllene, a natural bicyclic sesquiterpene, against cerebral ischemic injury. *J. Med. Food* **2013**, *16*, 471–480. [[CrossRef](#)]
67. Viveros-Paredes, J.M.; Gonzalez-Castaneda, R.E.; Gertsch, J.; Chaparro-Huerta, V.; Lopez-Roa, R.I.; Vazquez-Valls, E.; Beas-Zarate, C.; Camins-Espuny, A.; Flores-Soto, M.E. Neuroprotective Effects of beta-Caryophyllene against Dopaminergic Neuron Injury in a Murine Model of Parkinson's disease Induced by MPTP. *Pharmaceutics* **2017**, *10*, 60. [[CrossRef](#)]
68. Assis, L.C.; Straliotto, M.R.; Engel, D.; Hort, M.A.; Dutra, R.C.; de Bem, A.F. Beta-Caryophyllene protects the C6 glioma cells against glutamate-induced excitotoxicity through the Nrf2 pathway. *Neuroscience* **2014**, *279*, 220–231. [[CrossRef](#)]
69. Youssef, D.A.; El-Fayoumi, H.M.; Mahmoud, M.F. Beta-caryophyllene protects against diet-induced dyslipidemia and vascular inflammation in rats: Involvement of CB2 and PPAR-gamma receptors. *Chem. Biol. Interact.* **2019**, *297*, 16–24. [[CrossRef](#)]
70. Katsuyama, S.; Mizoguchi, H.; Kuwahata, H.; Komatsu, T.; Nagaoka, K.; Nakamura, H.; Bagetta, G.; Sakurada, T.; Sakurada, S. Involvement of peripheral cannabinoid and opioid receptors in beta-caryophyllene-induced antinociception. *Eur. J. Pain* **2013**, *17*, 664–675. [[CrossRef](#)]
71. Alberti, T.B.; Barbosa, W.L.; Vieira, J.L.; Raposo, N.R.; Dutra, R.C. (-)-beta-Caryophyllene, a CB2 Receptor-Selective Phytocannabinoid, Suppresses Motor Paralysis and Neuroinflammation in a Murine Model of Multiple Sclerosis. *Int. J. Mol. Sci.* **2017**, *18*, 691. [[CrossRef](#)] [[PubMed](#)]

72. Yoon, M.A.; Jeong, T.S.; Park, D.S.; Xu, M.Z.; Oh, H.W.; Song, K.B.; Lee, W.S.; Park, H.Y. Antioxidant effects of quinolone alkaloids and 2,4-di-tert-butylphenol isolated from *Scolopendra subspinipes*. *Biol. Pharm. Bull.* **2006**, *29*, 735–739. [CrossRef] [PubMed]
73. Choi, S.J.; Kim, J.K.; Kim, H.K.; Harris, K.; Kim, C.J.; Park, G.G.; Park, C.S.; Shin, D.H. 2,4-Di-tert-butylphenol from potato protects against oxidative stress in PC12 cells and mice. *J. Med. Food* **2013**, *16*, 977–983. [CrossRef] [PubMed]
74. Nair, R.V.R.; Jayasree, D.V.; Biju, P.G.; Baby, S. Anti-inflammatory and anticancer activities of erythrodiol-3-acetate and 2,4-di-tert-butylphenol isolated from *Humboldtia unijuga*. *Nat. Prod. Res.* **2018**, *26*, 1–4. [CrossRef] [PubMed]
75. Zhao, F.; Wang, P.; Lucardi, R.D.; Su, Z.; Li, S. Natural Sources and Bioactivities of 2,4-Di-Tert-Butyphenol and Its Analogs. *Toxins* **2019**, *12*, 35. [CrossRef]
76. Lushchak, V.I. Free radicals, reactive oxygen species, oxidative stress and its classification. *Chem. Biol. Interact.* **2014**, *224*, 164–175. [CrossRef]
77. Rahman, K. Studies on free radicals, antioxidants, and co-factors. *Clin. Interv. Aging* **2007**, *2*, 219–236.
78. Uttara, B.; Singh, A.V.; Zamboni, P.; Mahajan, R.T. Oxidative stress and neurodegenerative diseases: A review of upstream and downstream antioxidant therapeutic options. *Curr. Neuropharmacol.* **2009**, *7*, 65–74. [CrossRef]
79. Halliwell, B. Antioxidants in human health and disease. *Annu. Rev. Nutr.* **1996**, *16*, 33–50. [CrossRef]
80. Wang, C.Y.; Wang, S.Y.; Chen, C.T. Increasing antioxidant activity and reducing decay of blueberries by essential oils. *J. Agric. Food Chem.* **2008**, *56*, 3587–3592. [CrossRef]
81. Pinheiro, B.G.; Silva, A.S.B.; Souza, G.E.P.; Figueiredo, J.G.; Cunha, F.Q.; Lahlou, S.; da Silva, J.K.R.; Maia, J.G.S.; Sousa, P.J.C. Chemical composition, antinociceptive and anti-inflammatory effects in rodents of the essential oil of *Peperomia serpens* (SW.) Loud. *J. Ethnopharmacol.* **2011**, *138*, 479–486. [CrossRef] [PubMed]
82. Fonsêca, D.V.; Salgado, P.R.R.; de Carvalho, F.L.; Salvadori, M.G.S.S.; Penha, A.R.S.; Leite, F.C.; Borges, C.J.S.; Piuvezam, M.R.; Pordeus, L.C.d.M.; Sousa, D.P.; et al. Nerolidol exhibits antinociceptive and anti-inflammatory activity: Involvement of the GABAergic system and proinflammatory cytokines. *Fundam. Clin. Pharmacol.* **2015**, *30*, 14–22. [CrossRef] [PubMed]
83. Arbale, V.A.; Kamble, G.S.; Khatiwora, E.; Ghayal, N. Antioxidant capacity of leaves and stem of *Ehretia laevis*. *Int. J. Pharm.* **2011**, *3*, 149–151.
84. Tyagi, T.; Agarwal, M. Phytochemical screening and GC-MS analysis of bioactive constituents in the ethanolic extract of *Pistia stratiotes* L. and *Eichhornia crassipes* (mart.) solms. *J. Pharmacogn. Phytochem.* **2017**, *6*, 195–206.
85. Syad, N.A.; Rajamohamed, B.S.; Shunmugaiah, K.P.; Kasi, P.D. Neuroprotective Effect of the Marine Macroalga *Gelidiella Acerosa*: Identification of Active Compounds Through Bioactivity-Guided Fractionation. *Pharm Biol.* **2016**, *54*, 2073–2081. [CrossRef]
86. García-Argáez, A.N.; Apan, T.O.R.; Delgado, H.P.; Velázquez, G.; Martínez-Vázquez, M. Anti-inflammatory Activity of Coumarins from Decatropis Bicolor on TPA Ear Mice Model. *Planta Med.* **2000**, *66*, 279–281. [CrossRef]
87. Zahri, S.; Razavi, S.M.; Moatamed, Z. Antioxidant activity and cytotoxic effect of aviprin and aviprin-3'-O-D-glucopyranoside on LNCaP and HeLa cell lines. *Nat. Prod. Res.* **2012**, *26*, 540–547. [CrossRef]
88. Kang, T.J.; Lee, S.Y.; Singh, R.P.; Agarwal, R.; Yim, D.S. Anti-tumor activity of oxypeucedanin from *Ostericum koreanum* against human prostate carcinoma DU145 cells. *Acta Oncol.* **2009**, *48*, 895–900. [CrossRef]
89. Altameme, H.J.; Hameed, I.H.; Idan, S.A. Artemisia annua: Biochemical products analysis of methanolic aerial parts extract and anti-microbial capacity. *RJPBCS* **2016**, *7*, 1843–1868.
90. Costa, E.V.; Dutra, L.M.; De Jesus, H.C.R.; Nogueira, P.C.D.L.; Moraes, V.R.D.S.; Salvador, M.J.; Cavalcanti, S.C.D.H.; Santos, R.L.C.D.; Prata, A.P.D.N. Chemical composition and antioxidant, antimicrobial, and larvicidal activities of the essential oils of *Annona salzmannii* and *A. pickelii* (*Annonaceae*). *Nat. Prod. Commun.* **2011**, *6*, 907–912. [CrossRef]
91. Turkez, H.; Togar, B.; Tatar, A.; Geyikoglu, F. Cytotoxic and cytogenetic effects of  $\alpha$ -copaene on rat neuron and N2a neuroblastoma cell lines. *Biologia* **2014**, *69*, 936–942. [CrossRef]
92. Kundu, A.; Saha, S.; Walia, S.; Ahluwalia, V.; Kaur, C. Antioxidant potential of essential oil and cadinene sesquiterpenes of *Eupatorium adenophorum*. *Toxicol. Environ. Chem.* **2013**, *95*, 127–137. [CrossRef]

93. Ramesh, B.; Pugalendi, K.V. Antihyperlipidemic and antidiabetic effects of umbelliferone in streptozotocin diabetic rats. *Yale J. Biol. Med.* **2005**, *78*, 189–196.
94. Ramu, R.; Shirahatti, P.S.; Nanjunda, S.S.; Zameer, F.; Dhananjaya, B.L.; Nagendra, P.M.N. Correction: Assessment of In vivo Antidiabetic Properties of Umbelliferone and Lupeol Constituents of Banana (*Musa* sp. Var. Nanjangud Rasa Bale) Flower in Hyperglycaemic Rodent Model. *PLoS ONE* **2016**, *11*, e0151135. [CrossRef] [PubMed]
95. Sim, M.O.; Lee, H.I.; Ham, R.; Seo, K.I.; Kim, M.J.; Lee, M.K. Anti-inflammatory and antioxidant effects of umbelliferone in chronic alcohol-fed rats. *Nutr. Res. Pract.* **2015**, *9*, 364–369. [CrossRef]
96. Sigh, R.; Sigh, B.; Sigh, S.; Kumar, N. Umbelliferone—An antioxidant isolated from *Acacia nilotica* (L.) Willd. *Ex. Del. Food Chem.* **2009**, *120*, 825–830.
97. Seong, S.H.; Ali, M.Y.; Jung, H.A.; Choi, J.S. Umbelliferone derivatives exert neuroprotective effects by inhibiting monoamine oxidase A, self-amyloid $\beta$  aggregation, and lipid peroxidation. *Bioorganic Chem.* **2019**, *92*, 103293. [CrossRef]
98. Subramaniam, S.R.; Ellis, E.M. Neuroprotective effects of umbelliferone and esculetin in a mouse model of Parkinson’s disease. *J. Neurosci. Res.* **2013**, *91*, 453–461. [CrossRef]
99. Liang, S.; Chen, Z.; Li, H.; Cang, Z.; Yin, K.; Wu, M.; Luo, S. Neuroprotective effect of Umbelliferone against Cerebral ischemia/Reperfusion induced neurological deficits: In-vivo and in-silico studies. *J. Biomol. Struct. Dyn.* **2020**. [CrossRef]
100. Qakmak, Y.S.; Aktumsek, A.; Duran, A. Studies on antioxidant activity, volatile compound and fatty acid composition of different parts of *Glycyrrhiza echinata* L. *EXCLI J.* **2012**, *11*, 178–187.
101. Ng, T.B.; Liu, F.; Wang, Z.T. Antioxidative Activity of Natural Products from Plants. *Life Sci.* **2000**, *66*, 709–723. [PubMed]
102. He, W.; Chen, W.; Zhou, Y.; Tian, Y.; Liao, F. Xanthotoxol exerts neuroprotective effect via suppression of the inflammatory response in a rat model of focal cerebral ischemia. *Cell Mol. Neurobiol.* **2013**, *33*, 715–722. [PubMed]
103. Shalaby, N.M.M.; Abd-Alla, H.I.; Aly, H.F.; Albalawy, M.A.; Shaker, K.H.; Bouajila, J. Preliminary In Vitro and In Vivo Evaluation of Antidiabetic Activity of *Ducrosia anethifolia* boiss. and Its Linear Furanocoumarins. *BioMed Res. Int.* **2014**. [CrossRef]
104. Doungsaard, P.; Chansakaow, S.; Sirithunyalug, J.; Shang-Chian, L.; Wei-Chao, L.; Chia-Hua, L.; Kuan-Ha, L.; Leelapornpisid, P. In vitro Biological Activities of the Anti-aging Potential of *Dimocarpus longan* Leaf Extracts. *CMU J. Nat. Sci.* **2020**, *19*, 235–251.
105. Cascale, H.S.; Mullers, E.; Lindqvist, A. How the cell cycle enforce senescence. *Aging* **2017**, *9*, 2022–2023.
106. Mombach, J.C.M.; Bug, C.A.; Chaouiya, C. Modelling the onset of senescence at the G1/S cell cycle checkpoint. *BMC Genom.* **2014**, *15*, 1–11.
107. Gire, V.; Dulic’, V. Senescence from G2 arrest, revisited. *Cell Cycle* **2014**, *14*, 297–304.
108. Zhu, Y.; Armstrong, J.L.; Tchkonia, T.; Kirkland, J.L. Cellular senescence and the senescent secretory phenotype in age-related chronic diseases. *Curr. Opin. Clin.* **2014**, *17*, 324–328.
109. Campisi, J. Cancer, Aging and Cellular Senescence. *In Vivo* **2000**, *14*, 183–188. [PubMed]
110. Kumar, M.; Seeger, W.; Voswinckel, R. Senescence-associated Secretory Phenotype and Its Possible Role in Chronic Obstructive Pulmonary Disease. *Am. J. Respir. Cell Mol. Biol.* **2014**, *51*, 323–333. [PubMed]
111. Minamino, T.; Miyauchi, H.; Yoshida, T.; Tateno, K.; Kunieda, T.; Komuro, I. Vascular Cell Senescence and Vascular Aging. *J. Mol. Cell Cardiol.* **2004**, *36*, 175–183. [CrossRef] [PubMed]
112. Umran, N.S.S.; Mohamed, S.; Lau, S.F.; Ishak, N.I.M. *Citrus hystrix* leaf extract attenuated diabetic-cataract in STZ-rats. *J. Food Biochem.* **2020**, *44*, e13258. [PubMed]
113. Santiago, L.A.; Mayor, A.B. Prooxidant Effect of the Crude Ethanolic Leaf Extract of *Ficus odorata* Blanco Merr. In Vitro: Its Medical Significance. *Int. J. Biotechnol. Bioeng.* **2014**, *8*, 53–60.
114. Nurse, P. Checkpoint Pathways Come of Age. *Cell* **1997**, *91*, 865–867. [CrossRef]
115. Ezhevsky, S.A.; Ho, A.; Becker-Hapak, M.; Davis, P.K.; Dowdy, S.F. Differential Regulation of Retinoblastoma Tumor Suppressor Protein by G1 Cyclin-Dependent Kinase Complexes in Vivo. *Mol. Cell. Biol.* **2001**, *21*, 4773–4784.
116. Ezhevsky, S.A.; Nagahara, H.; Vocero-Akbani, A.M.; Gius, D.R.; Wei, M.C.; Dowdy, S.F. Hypo-phosphorylation of the retinoblastoma protein (pRb) by cyclin D:Cdk4/6 complexes results in active pRb. *Proc. Natl. Acad. Sci. USA* **1997**, *94*, 10699–10704.

117. Harbour, J.W.; Dean, D.C. The Rb/E2F pathway: Expanding roles and emerging paradigms. *Gene Dev.* **2000**, *14*, 2393–2409. [[CrossRef](#)]
118. He, G.; Thuillier, P.; Fischer, S.M. Troglitazone Inhibits Cyclin D1 Expression and Cell Cycling Independently of PPAR $\gamma$  in Normal Mouse Skin Keratinocytes. *J. Investig. Dermatol.* **2004**, *123*, 1110–1119. [[CrossRef](#)]
119. Hosooka, T.; Ogawa, W. A novel role for the cell cycle regulatory complex cyclin D1-CDK4 in gluconeogenesis. *J. Diabetes Investig.* **2015**, *7*, 27–28. [[CrossRef](#)]
120. Chang, C.; Su, H.; Zhang, D.; Wang, Y.; Shen, Q.; Liu, B.; Huang, R.; Zhou, T.; Peng, C.; Wong, C.C.; et al. AMPK-Dependent Phosphorylation of GAPDH Triggers Sirt1 Activation and Is Necessary for Autophagy upon Glucose Starvation. *Mol. Cell* **2015**, *60*, 930–940. [[CrossRef](#)]
121. Yang, Q.; Wang, B.; Gao, W.; Huang, S.; Liu, Z.; Li, W.; Jia, L. SIRT1 is downregulated in gastric cancer and leads to G1-phase arrest via NF- $\kappa$ B/Cyclin D1 signaling. *Mol. Cancer Res.* **2013**, *11*, 1497–1507. [[CrossRef](#)] [[PubMed](#)]
122. Zhou, S.; Li, M.T.; Jia, Y.Y.; Liu, J.J.; Wang, Q.; Tian, Z.; Liu, Y.T. Regulation of Cell Cycle Regulators by SIRT1 Contributes to Resveratrol-Mediated Prevention of Pulmonary Arterial Hypertension. *BioMed Res. Int.* **2015**, *2015*, 1–14. [[CrossRef](#)] [[PubMed](#)]
123. Omoregie, E.S.; Osagie, A.U. Effect of *Jatropha tanjoresis* leaves supplement on activities of some antioxidant enzymes, vitamins and lipid peroxidation in rat. *J. Food Biochem.* **2011**, *35*, 409–424. [[CrossRef](#)]
124. Omoregie, E.S.; Osagie, A.U. Phytochemical screening and anti-anaemia effect of *Jatropha tanjoresis* leaf in protein malnourished rats. *Plant. Arch.* **2007**, *7*, 509–516.
125. Shafaquat, N.; Syed, T.; Showkat, A.G. Glutathione-S-transferase, Superoxide Dismutase (GST, SOD) levels, Protein content and lipid Peroxidation in *Schizothorax plagiostomus* under the infection of *pomphorhynchus* in Nallah Sukhnag of Kashmir Valley. *Pakistan. J. Biol. Sci.* **2017**, *20*, 442–446.
126. AshokKumar, T. Antioxidants: New-generation therapeutic base for treatment of polygenic disorders. *Curr. Sci.* **2004**, *86*, 496–504.
127. Jonas, C.R.; Puckett, A.B.; Jones, D.P.; Griffith, D.P.; Szeszycki, E.E.; Bergman, G.F.; Furr, C.E.; Tyre, C.; Carlson, J.L.; Galloway, J.R.; et al. Plasma antioxidant status after high-dose chemotherapy a randomized trial of parenteral nutrition in bone marrow transplantation patients. *Am. J. Clin. Nutr.* **2000**, *72*, 181–189. [[CrossRef](#)]
128. Bahrami, S.; Jalali, M.H.; Jafari, A. Evaluation of hepatic antioxidant changes in ovine discroclosiosis. *J. Parasit. Dis.* **2015**, *39*, 766–769.
129. Deger, S.; Deger, Y.; Ertekin, A.; Gul, K.; Ozdal, N. Determination of the status of lipid peroxidation and antioxidant in Cattle infected with *Dictyocaulus viviparous*. *Turk. Parasitol.* **2008**, *32*, 234–237.
130. Siwela, A.H.; Motsi, L.R.; Dube, S. Alteration of some hepatic enzyme activities by gastrointestinal helminth parasite in domesticated ostriches. *Adv. Biores.* **2013**, *4*, 145–150.
131. Pranitha, A.; Lakshmi, P.K. Effect of pH on weakly acidic and basic model drugs and determination of their ex vivo transdermal permeation routes. *Braz. J. Pharm. Sci.* **2018**, *54*, e00070.
132. Persson, L.C.; Porter, C.J.H.; Charman, W.N.; Bergström, C.A.S. Computational Prediction of Drug Solubility in Lipid Based Formulation Excipients. *Pharm. Res.* **2013**, *30*, 3225–3237. [[CrossRef](#)] [[PubMed](#)]
133. Agarwal, A.; Roychoudhury, S.; Sharma, R.; Gupta, S.; Majzoub, A.; Sabanegh, E. Diagnostic application of oxidation-reduction potential assay for measurement of oxidative stress: Clinical utility in male factor infertility. *Reprod. Biomed. Online* **2017**, *34*, 48–57. [[CrossRef](#)]
134. Ortiz-Prado, E.; Dunn, J.F.; Vasconez, J.; Castillo, D.; Viscor, G. Partial pressure of oxygen in the human body: A general review. *Am. J. Blood Res.* **2019**, *9*, 1–14.
135. Donovan, L.; Welford, S.M.; Haaga, J.; LaManna, J.; Strohl, K.P. Hypoxia-implications for pharmaceutical developments. *Sleep Breath.* **2010**, *14*, 291–298. [[CrossRef](#)]
136. Hussain, K.; Ismail, Z.; Sadikun, A.; Ibrahim, P. Bioactive Markers Based Pharmacokinetic Evaluation of Extracts of a Traditional Medicinal Plant, *Piper sarmentosum*. *Evid.-Based Complement. Altern. Med.* **2011**, *980760*, 1–7. [[CrossRef](#)]
137. Smith, D.A.; Beaumont, K.; Maurer, T.S.; Di, L. Volume of Distribution in Drug Design. *J. Med. Chem.* **2015**, *58*, 5691–5698. [[CrossRef](#)]

138. Babu, S.; Jayaraman, S. An update on  $\beta$ -sitosterol: A potential herbal nutraceutical for diabetic management. *Biomed. Pharmacother.* **2020**, *131*, 110702. [[CrossRef](#)] [[PubMed](#)]
139. Liu, H.; Yang, G.; Tang, Y.; Cao, D.; Qi, T.; Qi, Y.; Fan, G. Physicochemical characterization and pharmacokinetics evaluation of  $\beta$ -caryophyllene/ $\beta$ -cyclodextrin inclusion complex. *Int. J. Pharm.* **2013**, *450*, 304–310. [[CrossRef](#)]



© 2020 by the authors. Licensee MDPI, Basel, Switzerland. This article is an open access article distributed under the terms and conditions of the Creative Commons Attribution (CC BY) license (<http://creativecommons.org/licenses/by/4.0/>).